University of Alberta

Carbonic Anhydrase II Promotes Cardiomyocyte Hypertrophy

by

Brittany Fielding Brown

A thesis submitted to the Faculty of Graduate Studies and Research
in partial fulfillment of the requirements for the degree of

Master of Science

Department of Physiology

Spring 2012
Edmonton, Alberta

I am truly grateful for all of the support and encouragement I received from my family. I dedicate this thesis to my parents, Chris and Gail Brown, my sister, Morgan Brown, and my boyfriend, Curtis Wyllie.

Abstract

Cardiac hypertrophy is maladaptive remodeling of the myocardium that often progresses to heart failure. The hypertrophic transport metabolon consists of membrane transporters implicated in hypertrophy, and substrates for these transporters are provided by the catalytic action of carbonic anhydrase II (CAII). CAII inhibition prevents and reverts cardiomyocyte hypertrophy *in vitro*, suggesting that CAII is an important protein in the development of hypertrophy. To explore this further, neonatal rat ventricular myocytes (NRVMs) were transduced with adenoviral constructs to over-express wild type or catalytically inactive CAII. Upon treatment with phenylephrine, NRVMs over-expressing catalytically inactive CAII exhibited reduced cardiac remodeling associated with hypertrophy. Cardiomyocytes isolated from a line of mice with a null mutation in the CAII gene were also protected from hypertrophic stimulation. The findings of these studies support the importance of CAII in the promotion of cardiac hypertrophy, and may potentially lead to new therapeutic strategies for heart failure.

Acknowledgements

First and foremost, I would like to thank Dr. Joe Casey for the opportunity to be a graduate student in his lab. His leadership and teachings have helped me to grow as a scientist and learn how to approach many of the challenges that accompany this field. I genuinely valued his patience and support during the past three years.

I have had the pleasure of working with a number of past and present members of the Casey lab who have all been wonderful colleagues and friends. The efforts of Anita Quon and Daniel Sowah in the development of my research, as well as their guidance and patience, are much appreciated. I am also very thankful for discussions with Arghya Basu, Shirley Mazor, Gonzalo Vilas, Pamela Bonar, Danielle Johnson, Sampath Loganathan, and Eylem Baspinar.

I would like to take this opportunity to thank my committee, Dr. Larry Fliegel and Dr. Elaine Leslie, for their guidance and support. Jamie Boisvenue, Carrie Soltys, and Amy Barr from Dr. Jason Dyck's lab were very helpful with my research, and I appreciate the discussions we had. Many other past and present members of the departments of Physiology and Biochemistry have been great resources as well as great friends, and I will fondly remember the times we spent together. In particular, I would like to thank Kate Witkowska for her friendship and encouragement, and for all the great times we had in and out of the lab!

My family has always been there for me and supported me in my endeavours, I can't possibly thank them enough. The love and support of Curtis Wyllie has meant the world to me, and I'm truly grateful for his constant reassurance and faith in me.

Finally, I would like to acknowledge the Alberta Heritage Foundation for Medical Research for their financial support.

Table of Contents

List of Tables

List of Figures

List of Symbols, Nomenclature, Abbreviations

4-MI	4-methylimidazole
A	blood flow velocity through mitral valve during the atrial kick/left atrial systole
Acetyl-CoA	acetyl-coenzyme A
ACTZ	acetazolamide
AdCAIIM	an adenovirus encoding for CAII-V143Y and GFP
AdCAIIWT	an adenovirus encoding for wild type CAII and GFP
AdGFP	an adenovirus encoding for GFP
AE	anion exchanger
AE3c	anion exchanger isoform 3 cardiac
AE3fl	anion exchanger isoform 3 full length
Akt	protein kinase B
ANGII	angiotensin II
ANP	atrial natriuretic peptide
AT_1R	angiotensin II type 1 receptor
ATF-2	activating transcription factor-2
ATP	adenosine triphosphate
BDM	2,3-butanedione monoxime
BNP	brain natriuretic peptide
BP	blood pressure
bpm	beats per minute
BW	body weight
C terminus	carboxyl terminus
CA	carbonic anhydrase
caii$^{-/-}$ mice	mice with a null mutation in the CAII gene
CAII-H64A	an N-terminal CAII mutant unable to shuttle H^+
CAII-V143Y	a catalytically inactive CAII mutant
CAL	coronary artery ligation
cAMP	cyclic adenosine monophosphate

CARP	carbonic anhydrase related protein
CBE	Cl^-/HCO_3^- exchanger
cDNA	complementary DNA
cGMP	guanosine 3'-5'-cyclic monophosphate
CNP	C-type natriuretic peptide
CO_2	carbon dioxide
CVD	cardiovascular disease
Cx43	connexin 43
d	diastolic
DAG	diacyl glycerol
DMEM	Dulbecco's Modified Eagle's Medium
DNA	deoxyribonucleic acid
DRA	downregulated in adenoma, SLC26A3
DTT	dithiothreitol
E	blood flow velocity through mitral valve during the E wave/left ventricular diastole
E'	E wave mitral valve tissue motion
EC	extracellular loop
EF	ejection fraction
EGFP	enhanced green fluorescent protein
EGFP-e1-CAII	a fusion protein with enhanced green fluorescent protein at the N-terminal end of NBCe1-A and CAII at the C-terminal end
eIF	eukaryotic initiation factor
ERK	extracellular signal-regulated kinase
ET-1	endothelin-I
ETZ	ethoxyzolamide
FS	fractional shortening
GAPDH	glyceraldehyde 3-phosphate dehydrogenase
GFP	green fluorescent protein
GPCR	G-protein coupled receptor

GSK3	glycogen synthase kinase 3
GST	glutathione S-transferase
GST-AE1EC3	a glutathione S-transferase fusion protein of the third extracellular loop of AE1
GST-AE1EC4	a glutathione S-transferase fusion protein of the fourth extracellular loop of AE1
GST-Ct	a glutathione S-transferase fusion protein with the last 33 residues of AE1
GTP	guanosine triphosphate
HDAC	histone deactylase
HEK293 cells	human embryonic kidney 293 cells
HEPES	4-(2-hydroxyethyl)-1-piperazineethanesulfonic acid
HIF	hypoxia-inducible factor
HR	heart rate
HRP	horseradish peroxidase
HW	heart weight
IGF	insulin growth factor
IgG	immunoglobulin G
IL	interleukin
IP3	inositol 1,4,5-triphosphate
ITS	insulin-transferrin-selenium
IVS	interventricular septum
JNK	c-Jun NH_2-terminal kinase
kDa	kilodalton
LVID	left ventricular internal diameter
LVM	left ventricular mass
LVPW	left ventricular posterior wall
MAPK	mitogen activated protein kinase
MCT	monocarboxylate transporter
MEF-2	myocyte enhancer factor-2
MHC	myosin heavy chain

MHz	megahertz
MI	myocardial infarction
MLC	myosin light chain
MLK	mixed lineage kinase
MMP	matrix metalloproteinase
MOI	multiplicity of infection
mRNA	messenger ribonucleic acid
mTor	mammalian target of rapamycin
MV	mitral valve
N terminus	amino terminus
NBC	$Na^+HCO_3^-$ co-transporter
NCBE	Na^+-Cl^-/HCO_3^- exchanger
NCX	Na^+/Ca^{2+} exchanger
NDCBE	Na^+-driven Cl^-/HCO_3^- exchanger
NFAT	nuclear factor of activated T-cells
NFκB	nuclear factor kappa-light-chain-enhancer of activated B cells
NHE	Na^+/H^+ exchanger
NPR	natriueretic peptide receptor/guanylyl cyclase
NRVM	neonatal rat ventricular myocytes
P	plasmid
PBS	phosphate-buffered saline
PCR	polymerase chain reaction
PDK-1	3-phosphoinositide dependent kinase-1
PE	phenylephrine
PGK-1	cGMP-dependent protein kinase-1
PI3K	phosphoinositide 3-kinase
PIP2	phosphatidylinositol 4,5 biphosphate
PIP3	phosphatidylinositol 3,4,5 triphosphate
PKA	protein kinase A
PKC	protein kinase C

PLC	phospholipase C
qPCR	quantitative real-time PCR
RNA	ribonucleic acid
RTK	receptor tyrosine kinase
s	systolic
S.E.M.	standard error of the mean
SAPK	stress-activated MAPK
SDS	sodium-dodecyl sulphate
SERCA	sarco-endoplasmic reticulum Ca^{2+}-ATPase
SLC	solute carrier
SLC4-Ct	carboxy terminus of an SLC4 protein
SLC4-GST-Ct	a glutathione S-transferase fusion protein with the Ct of an SLC4 protein
STAS	Sulfate Transporters and Anti Sigma antagonists
TAC	transverse aortic constriction
TBS	tris-buffered saline
TCA	tricarboxylic acid
TEMED	N,N,N',N',-tetramethylenediamine
TNF	tumour necrosis factor
α-ADR	α-adrenergic receptor
β-ADR	β-adrenergic receptor
μM	micromolar

Chapter 1: General Introduction

1.1 Thesis Overview

The objective of this thesis is to explore the role of carbonic anhydrase II (CAII) in cardiomyocyte hypertrophy. Hypertrophic markers (cell size, protein synthesis, and hypertrophic gene expression) were monitored in neonatal rat ventricular myocytes over-expressing wild type or catalytically inactive CAII. Also, cardiovascular parameters were characterized from a line of mice with a null mutation in the *caii* gene, and the same hypertrophic markers were monitored in cardiomyocytes isolated from these mice in the presence of hypertrophic agonists. Specifically, we wanted to determine the effect of over-expressing CAII, or ablation of CAII, on phenylephrine (PE)-induced hypertrophy in cardiomyocytes.

Cardiovascular pH regulation has been implicated in several cardiovascular pathologies, including cardiomyocyte hypertrophy, therefore this introduction will begin with a description of the transmembrane proteins and carbonic anhydrases involved in pH regulation in the heart. Carbonic anhydrases catalyze the production of substrates for several pH regulatory transport proteins, so a review of the bicarbonate transport metabolon is included. Important aspects of cardiac hypertrophy, including cardiac remodeling and major pathways in the hypertrophic cascade, are also discussed. The final section will discuss the concept of a hypertrophic transport metabolon, and the promotion of cardiomyocyte hypertrophy through the interaction of CAII with other pH regulatory proteins.

1.2 Cardiovascular pH Regulation

The heart is a muscle, and therefore requires energy by means of metabolism in order to function. One outcome of cellular metabolism is an increase in intracellular acid. The maintenance of a resting pH of 7.2 requires the removal of extra intracellular H^+, in order to prevent acute contractile depression, alterations in Ca^{2+} signaling, and arrhythmias. Cardiovascular pH is regulated

mainly by transport proteins in the plasma membrane and gap junctions, and by intracellular buffers (Fig. 1.1).

1.2.1 Na^+H^+ Exchangers

Na^+H^+ exchangers (NHEs) are electroneutral transmembrane proteins that exchange one H^+ for one Na^+. Since they respond to decreases in pH, NHEs likely account for most of the acid extrusion activity in cells (36). They have 12 transmembrane domains, a hydrophobic amino terminus, and a large cytosolic C-terminus that is involved in regulation of NHE activity (36). Of the ten isoforms of NHE, NHE1 is the most ubiquitously expressed, and is the predominant isoform expressed in the heart (84). The cytosolic domain of NHE1 consists of phosphorylation sites, as well as sites for interaction with calmodulin, and calcineurin homologous protein, all of which activate the transporter (36). The other NHE isoforms are expressed in a variety of tissues, including the intestine, kidney, gastrointestinal tract, skeletal muscle, testis and brain (50). NHE6-9 are also ubiquitously expressed, but on intracellular membranes such as the Golgi, where they function to regulate organelle pH (36).

NHE1 activity has been implicated in the cardiovascular pathologies, specifically ischemia/reperfusion, and cardiac hypertrophy. During ischemia, blood flow to the heart is blocked, resulting in hypoxia and increases in intracellular lactate and $[H^+]$. Under acidotic conditions, NHE1 mRNA transcript levels are elevated, and its transport activity increased in order to restore physiological pH (36). Increased intracellular Ca^{2+} resulting from sustained NHE1 activity activates several pathways that promote cardiac hypertrophy, which will be discussed in more detail in a later section.

1.2.2 $Na^+HCO_3^-$ Co-Transporters

$Na^+HCO_3^-$ co-transporters (NBC) are members of the SLC4A family and important transporters of bicarbonate. The five isoforms (NBCe1, NBCe2, NBCn1, NDCBE, and NCBE) vary in terms of electrogencity, stoichiometry, and

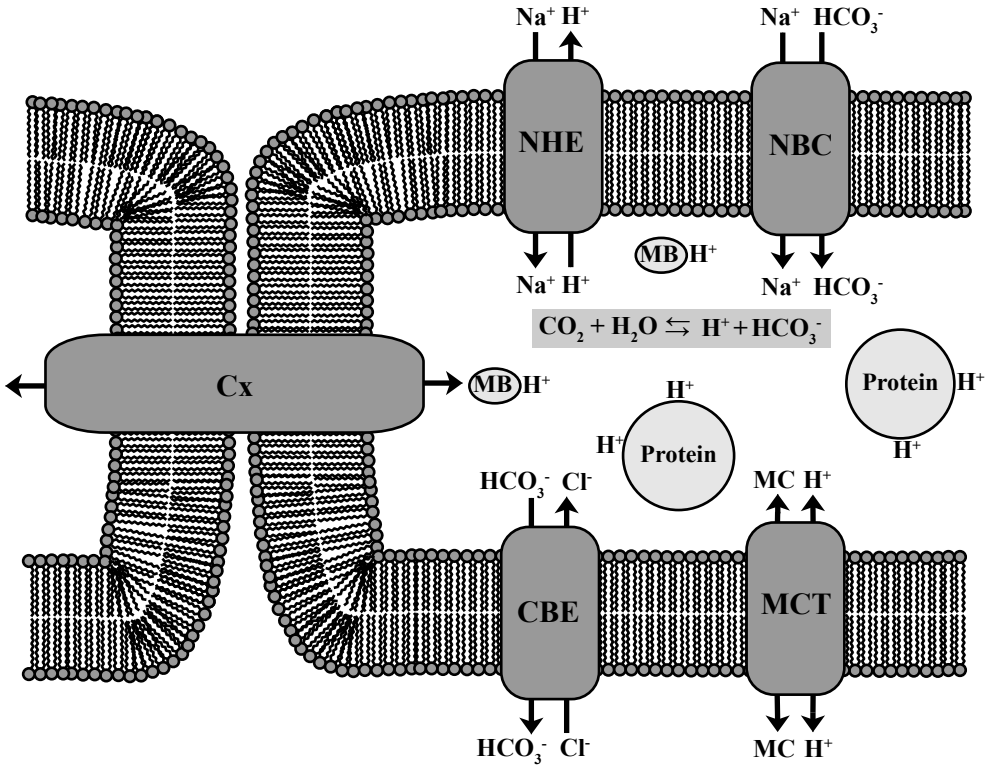

Figure 1.1. Cardiovascular pH Regulation

Cardiovascular pH is regulated by membrane transport activity and intracellular buffering (133). NHE1 and NBC transporters function to alkalinize the myocyte by H^+ extrusion and HCO_3^- loading, respectively. Cl^-/HCO_3^- exchangers (CBE) extrude HCO_3^-, thereby acidifying the myocyte. MCT activity is dependent on monocarboxylate (MC) levels within the myocyte, and can be either acid extruders or acid loaders. H^+ can also be transported through connexin channels (Cx) at gap junctions between myocytes. Intracellular buffering is the summation of carbonic buffering ($CO_2 + H_2O \leftrightarrow H^+ + HCO_3^-$) and intrinsic buffering. Intrinsic buffering is the binding of H^+ to amino acid side chains and phosphates on intracellular proteins, or to low molecular weight mobile buffers (MB).

tissue distribution, but all mediate the cotransport of Na^+ and HCO_3^- (107, 117). NDCBE transports Cl^- in addition to Na^+ and HCO_3^-, and the predominant substrates of NCBE are inconclusive (107). Both NBCe1 and NBCe2 are electrogenic and expressed in the heart, with a stoichiometry of 2 HCO_3^- per Na^+ (117). NBCn1 is electroneutral and also expressed in the heart. All three isoforms participate in pH regulation in the heart through the transport of HCO_3^- into myocytes, resulting in intracellular alkalinization (107, 118). Changes in pH are one of the ways NBC activity is regulated in tissues; an increase in metabolic acidosis upregulated NBC activity in the kidney, while metabolic alkalosis down-regulated NBC activity (118). While the role of NBCs in cardiovascular pathologies is yet to be elucidated, there is some evidence of an upregulation of NBCe1 in human cardiomyopathic hearts, and administration of an anti-NBCe1 antibody protected the systolic and diastolic functions of the heart during ischemia/reperfusion (51). NBCe1 and NBCn1 are upregulated in cardiac hypertrophy (143), suggesting that NBCs might be a potential target in reducing heart failure, but it is difficult to move forward with this research without specific NBC inhibitors (10).

1.2.3 Cl^-/HCO_3^- Exchangers

Cl^-/HCO_3^- exchangers are encoded for by two different families: SLC4 and SLC26. Those in the SLC4 family are called anion exchangers (AE), of which there are three isoforms (AE1, AE2, and AE3). The AEs are electroneutral transporters, consisting of a membrane domain that facilitates transport and an N-terminal cytoplasmic domain (28). They have three main functions: HCO_3^- metabolism, pH regulation, and regulation of cell volume (25). There are two AE1 transcripts, one expressed in erythrocytes (eAE1) and one expressed in the basolateral membrane of α-intercalated cells of the renal collecting duct (kAE1) (28). AE2 is more widely expressed, particularly in gastric parietal cells, the basolateral membrane of choroid plexus epithelial cells, and throughout the nephron (28). AE3 is expressed in the brain, heart and retina, and, like AE1, has two transcripts: AE3 full length (AE3fl) and AE3 cardiac (AE3c) (28).

Five of ten members of the SLC26 family have been established as bicarbonate transporters: SLC26A3, 4, 6, 7, and 9 (28). They generally exist as dimers, and are widely expressed in the body (28). The transport stoichiometry of these transporters remains indefinite, although there is evidence to suggest that SLC26A3, 6, and 7 are electrogenic, while SLC26A4 is electroneutral (28). Little is known about SLC26A9 (28). All SLC26 proteins contain a STAS (Sulfate Transporters and Anti Sigma antagonists) domain, which participates in protein-protein interactions (28). In the heart, both SLC26A3 and 6 are expressed, SLC26A6 in fact being the most predominantly expressed bicarbonate transporter in the heart (5). Implications of anion exchangers in cardiomyocyte hypertrophy will be discussed in a later section.

1.2.4 Monocarboxylate Transporters

Under hypoxic conditions, pyruvate is reduced in order to oxidize electron carriers so they can continue to participate in glycolysis. This results in an increase in intracellular lactate, as well as $[H^+]$ which needs to be removed from the cell to prevent acidosis and the inhibition of glycolysis. On the other hand, under normoxic conditions, lactate can be transported into the cell and converted to pyruvate to fuel gluconeogenesis or the tricarboxylic acid (TCA) cycle. Of the fourteen isoforms of monocarboxylate transporters (MCT), which belong to the SLC16 family, MCT1-4 are the only isoforms that have been experimentally shown to co-transport H^+ and lactate, or other monocarboxylates, such as pyruvate and ketone bodies (41). They are ubiquitously expressed in tissues, particularly in muscle and brain which consume significant amounts of energy (41). While there is no detailed structure of an MCT, they are thought to have twelve transmembrane domains, and intracellular N and C termini (76). MCTs are regulated at the level of transcription and translation, and they require the coexpression of an accessory protein for correct functional expression (76). In the heart, the presence of MCT1 and MCT2 was confirmed at the mRNA and protein expression level (76). MCT1 expression in the heart increases after ischemia and reperfusion, which is likely in order to restore cardiac pH (73).

1.2.5 Gap Junctions

Modest changes in pH, within a range of 6.9-7.25, are mostly regulated by gap junctions between myocytes (133). The connexin43 (Cx43) channel is the predominant channel expressed in gap junctions in ventricular myocytes, and it allows the transmission of H^+ between adjacent cells in the presence of a H^+ gradient (133). While this is an efficient method of pH regulation within a small range of pH, in more severe acidic or alkaline conditions the permeability of H^+ through Cx43 channels is reduced (133). Chronic acidosis can actually induce junctional remodeling, and cause Cx43 removal from gap junctions (133). This is likely a protective measure to prevent severe changes in pH from spreading to adjacent myocytes (133).

1.2.6 Intracellular pH Buffering

Cardiovascular pH is also regulated by intracellular H^+ buffering in myocytes, which is a summation of carbonic buffering and intrinsic buffering (133). Carbonic buffering is the generation of CO_2 and H_2O from H^+ and HCO_3^-, while intrinsic buffering is the binding of H^+ to amino acid side chains and phosphates on intracellular proteins (134). Proteins generally have low intracellular mobility, therefore the buffering of H^+ slows its diffusion in the cytosol significantly (134). Low molecular weight cytoplasmic H^+ carrier molecules, such as carnosine derivatives, are also able to bind H^+-ions and diffuse them throughout the cell, as well as between the cytosol and the sarcolemma (134). Despite this, the diffusion of H^+ in the cytosol is still two orders of magnitude slower than in water (134).

1.2.7 Carbonic Anhydrases

1.2.7.1 Structure and Function

Carbonic anhydrases (CA) are metalloenzymes that catalyze the hydration of CO_2 into H^+ and HCO_3^-. They are ubiquitously expressed in prokaryotes and

eukaryotes, and have evolved from five different gene families: α-, β-, γ-, δ-, and ζ- (34). α-CAs are found in vertebrates, bacteria, algae, and green plants, and are able to catalyze reactions other than just CO_2 hydration, although the physiological relevance of this is unknown (93). Both β- and γ-CAs are found in plants, bacteria, and Archaea (34, 110), while δ- and ζ-CAs are found in marine diatoms (60, 142). While all of the families are metalloenzymes, the oligomeric structure and the metal ion at the active site vary: α-, β-, and δ-CAs use Zn(II) (93), γ-CAs use primarily Fe(II) (34), and ζ-CAs use Cd(II) (60).

There are at least 16 isozymes of α-CA present in mammals. These include isozymes that are cytosolic (CAI, CAII, CAIII, CAVII, and CAXIII), membrane-associated (CAIV, CAIX, CAXII, CAIXIV, and CAXV), mitochondrial (CAVA and CAVB), and secreted in saliva (CAVI) (45). There are also three acatalytic CA-related proteins (CARP XIII, CARP X, and CARP XI) (93). The catalytic activities and tissue distribution vary between the isozymes, CAII having the highest turnover rate of approximately 10^6 s^{-1}.(72) CAIV is affixed to the extracellular surface of plasma membranes by a glycosylphosphatidylinositol anchor (87, 140), while CAXIV is anchored to the extracellular surface of plasma membranes by a transmembrane segment (80). In the heart, five isozymes of CA are present, which include: cytosolic CAII, membrane-associated CAIV, CAIX, and CAXIV, and mitochondrial CAVB (38, 112, 114, 139).

As mentioned, α-CAs contain a Zn(II) ion in the bottom of the active site of the enzyme, which is coordinated by three histidine ligands (93). The number and type of protein ligands can vary between CA families (93). CO_2 binds to the hydrophobic pocket of the enzyme, and is attacked by an hydroxide ion bound to the Zn(II) ion (93). The resulting bicarbonate ion is displaced by a water molecule, and a proton transferred to the environment in order to return CA to its basic, active state (93).

$$EZn^{2+}\text{-}OH^- + CO_2 \leftrightarrows EZn^{2+}\text{-}HCO_3^- \leftrightarrows EZn^{2+}\text{-}OH_2 + HCO_3^-$$

$$EnZn^{2+}\text{-}OH_2 \leftrightarrows EZn^{2+}\text{-}OH^- + H^+$$

The proton transfer from the zinc-bound water to the exogenous buffer is mediated by a His64 residue (16). Mutation of His64 in CAII to an alanine resulted in a 20-50 fold decrease in the H^+ transfer rate (16). The activity of the CAII H64A mutant was restored by the presence of exogenous H^+ donors/acceptors, such as derivatives of carnosine or imidazoles (16, 74). This is likely due to the binding of imidazoles, such as 4-methylimidazole (4-MI), close to the imidazole ring of His64 in CAII, where they can act as an intermediary for proton transfer (74). It is interesting to note that increasing amounts of 4-MI are able to almost saturate the activity of CAIII, which is the least catalytically efficient CA and has a lysine instead of a histidine at position 64 (7).

CAs play an important role in a number a biological pathways, including respiration, photosynthesis, biosynthetic pathways (such as gluconeogenesis, ureagenesis, and lipogenesis), electrolyte secretion, and pH regulation. While some of these metabolic processes require the CAVA/B- or CAII-catalyzed generation of HCO_3^- for the conversion of pyruvate to oxaloacetate, many produce CO_2 and H^+ as waste products, which then need to be excreted from the body (133). Waste H^+ is buffered by intracellular HCO_3^-, generating more CO_2 (133). The plasma membrane is highly permeable to CO_2, thereby allowing CO_2 to diffuse out of metabolic tissues (133). Some of this CO_2 is hydrated by extracellular CAs to prevent accumulation of CO_2 outside the cell (133). Protons, bicarbonate, and any remaining CO_2 diffuse to the bloodstream, and CO_2 diffuses into erythrocytes where it is hydrated by cytosolic CAs catalyze due to its low solubility in blood (133). NHEs, NBCs, and AEs in the erythrocyte plasma membrane transport H^+ and HCO_3^- into the bloodstream, to prevent their accumulation in the cell (25). Upon reaching the lungs, the low P_{CO_2} drives the production of CO_2 in the plasma, catalyzed by CAs, which leaves the plasma and is expelled by the lungs (25).

CA deficiencies in humans are rare, and to date there is only one disease caused by a CA deficiency: CAII deficiency syndrome. This disease is associated with renal tubular acidosis, osteopetrosis, and cerebral calcification, although the severity of the manifestation of these conditions depends on the mutation causing

the deficiency (116). So far, bone marrow or stem cell transplantation to halt progression of the osteoporosis and cerebral calcification are the only treatments available (1). There are cases of CAI deficiency as well, but no clinical abnormalities were present in these individuals (116).

1.2.7.2 Inhibitors and Activators

The manipulation of CA activity in the treatment of numerous human diseases has been extensively studied for decades. CAs are sensitive to inhibition by sulphonamides and sulphamates, which bind to the Zn(II) ion by substituting the non-protein zinc ligand (e.g. H_2O) to generate a tetrahedral adduct (127). The isozymes vary in their affinity for the different sulphonamides and sulphamates, except for CAIII, which is not susceptible to inhibition by these compounds (127). Despite the abundance of CA inhibitors, there is lack of isozyme-specific inhibitors, therefore there is often non-specific inhibition of CAs that results in undesired side effects (127). One solution is the design of inhibitors to be membrane-impermeant, which would allow only specific interactions with membrane-associated CAs (127).

CA inhibitors were first used as diuretics to treat edema in the 1950s, specifically acetazolamide (ACTZ) (Diamox), ethoxyzolamide (ETZ) (Cardrase), methazolamide, and dichlorophenamide (83, 127). Inhibition of CA in the kidneys reduces HCO_3^-, Na^+, and K^+ reabsorption, leading to retention of water in urine (128). These CA inhibitors are also used to treat glaucoma, which is characterized by an increase in intraocular pressure that causes damage to the optic nerve and eventually blindness (127). Inhibition of CAII in the eye reduced bicarbonate and aqueous humour secretion, and intraocular pressure by 25-30% (127). Topiramate and Zonisamide, two CA inhibitors used in anti-epileptic drugs, were found to have potential as anti-obesity drugs in that they inhibit the mitochondrial CA isozymes that provide bicarbonate to pyruvate in lipogenesis (39, 98). CA isozymes in osteoclasts may also be targeted to prevent osteoporosis (105). Finally, CAs have been demonstrated to be important in the growth and virulence

of certain pathogens, and inhibition may lead to the production of antimalarial, antituberculosis, and antifungal drugs (127).

Sulphonamides are being studied in their anti-cancer effects through the inhibition of CAIX (94). The hypoxia that occurs in tumours prevents the hydroxylation of hypoxia-inducible factor α (HIFα), which in turn prevents its degradation. HIFα translocates to the nucleus where it dimerizes with HIFβ to form an active transcription factor that binds to the hypoxia response element in target genes (94). One of these target genes is CAIX, which generates extracellular acidosis in hypoxic tissues and provides bicarbonate for metabolic processes (94). Derivative 17 is a fluorescent sulphonamide that only binds to CAIX under hypoxic conditions, and therefore may be used in tumour imaging (127). Derivative 18 is a membrane-impermeant sulphonamide that targets CAIX, and therefore may not cause the side effects associated with inhibiting intracellular CAs (127).

The effects of CA activators, such as phenylalanine, histamine, and carnosine, have also been studied in the treatment of disease (126). CA activation may play a role in increasing synaptic efficiency, and therefore be a possible therapy for Alzheimer's disease (126). Research on CA activators is still relatively new, but the potential for pharmacological derivatives that improve spatial learning and memory is there.

1.3 The Bicarbonate Transport Metabolon

Metabolons and substrate channeling are established concepts present in a number of biological systems, one of the most well-known being the TCA cycle (121). A metabolon is a complex of enzymes in a linked metabolic pathway that acts to maximize substrate flux, or channeling, by moving substrate from the active site of one enzyme to the next (75, 121). In the TCA cycle, disorganization in the mitochondrial matrix of the enzymes involved, particularly oxaloacetate, would not account for the rate of oxidization of acetyl-coenzyme A (CoA) (121). The physical interactions later discovered between the enzymes in the TCA cycle

further substantiated the presence of a metabolon (121). Metabolons in other metabolic pathways have been identified, including glycolysis, and the urea cycle (104). This section will describe metabolons that exist between carbonic anhydrases and several transmembrane proteins that contribute to intracellular pH regulation.

1.3.1 Anion Exchanger/Carbonic Anhydrase II Interactions

The Cl^-/HCO_3^- exchange activity of AE1 and the production of HCO_3^- through the hydration of CO_2 by CAII triggered the idea that AE1 and CAII might form a complex in order to localize substrate at the plasma membrane and increase transport efficiency (52). This notion was tested in a series of experiments analyzing possible physical and functional interactions. First, immunofluorescence exposed tomato lectin-mediated clustering of both AE1 and CAII, suggesting a physical interaction between the two proteins. This was reinforced by experiments revealing that CAII cosolubilized and coimmunoprecipiated with AE1 (137). Solid phase binding assays showed that AE1, and a glutathione S-transferase fusion protein with the last 33 residues of AE1 (GST-Ct), bound to immobilized CAII. This was also observed with affinity blotting and affinity chromatography using GST-Ct and CAII. These experiments demonstrate that a physical interaction exists between AE1 and CAII, and it occurs via the C terminus of AE1.

Further experiments using peptide competition, as well as truncation and point mutations, pinpointed the location of the binding site on the Ct of AE1 to an acidic motif, DADD, that was required for CAII binding (138). The AE1 binding site on CAII was localized to the first 17 residues of the protein, which constitute a basic region of the amino terminus (136). This was discovered with the loss of GST-Ct binding to CAII when several histidine residues and one lysine residue within these 17 residues were mutated to analogous residues in CAI, which doesn't bind AE1. Interestingly, the DADD sequence was found to be an activator of human CAII, indicating that the binding of AE1 to CAII facilitates the catalysis and formation of bicarbonate (113). This was not observed with human CAI or

CAIV, both of which don't have a region of histidines to bind to the DADD sequence on AE1 (113).

The transport activity of AE1 in transfected human embryonic kidney 293 (HEK293) cells was reduced by 50-60% when endogenous CAII was inhibited by acetazolamide (122). Mutation of the CAII binding site on AE1 reduced transport, which was not rescued by over-expression of CAII. AE1 activity was also reduced by the presence of a catalytically inactive CAII, CAII-V143Y, and the same effect was observed in AE2 and AE3c. In experiments where CAII was fused to the C terminus of AE1, wild type CAII didn't increase the activity of AE1, but CAII-V143Y reduced the transport of Cl^- by 60% (119). These experiments demonstrate that a physical interaction with CAII is essential for maximal transport activity of anion exchangers, and therefore support the existence of a bicarbonate transport metabolon (Fig. 1.2).

The presence of CAII is also important in the formation of pH microdomains around AE1 (47). Inhibition of CAII, using ETZ, suppresses the transport rate and the formation of a pH microdomain around AE1 (47), which further supports the idea of a bicarbonate transport metabolon. CAII activity generates H^+ and HCO_3^-, therefore the presence of CAII at the plasma membrane, bound to AE1, maximizes HCO_3^- extrusion. Since H^+ diffusion is slow in the cytosol, CAII activity produces a H^+ microdomain at the active site of AE1 (47). CAII inhibition therefore causes uncatalyzed production of H^+ and HCO_3^- throughout the cytosol, preventing the pH microdomain formation (47).

1.3.2 Anion Exchanger/ Carbonic Anhydrase IV, IX, and XIV Interactions

A physical interaction between anion exchangers and CAII opened up the possibility of interactions between anion exchangers and other carbonic anhydrases. In transfected HEK293 cells, expression of CAII-V143Y inhibited the transport activity of AE1, AE2, AE3, as previously described, but transport was restored by expression of CAIV (122). GST pull-down assays determined that

CAIV binds to the fourth extracellular loop of AE1, which is the largest extracellular loop in the protein. In this experiment, GST fusion proteins of the third and fourth extracellular loops (EC3 and EC4) of AE1 (GST-AE1EC4 and GST-AE1EC3, respectively) were immobilized on glutathione Sepharose resin, and cell lysates of CAIV transfected cells were applied. Immunoblots of the eluted proteins revealed that GST-AE1EC4 pulled down approximately 10-fold more CAIV than GST-AE1EC3 or GST alone. Whether CAIV binds to EC4 of AE2 and AE3 is unknown, since these two anion exchangers differ structurally from AE1 in that EC3 is the largest loop and is the one glycosylated. It is likely though that a physical interaction exists between these proteins and CAIV, because of the functional interaction described above.

The first functional and physical interaction between bicarbonate transporters and a transmembrane carbonic anhydrase was discovered between anion exchangers and CAIX (79). When coexpressed in HEK293 cells, CAIX coimmunoprecipitated with AE1, AE2, and AE3 (79). Coimmunofluorescence showed that CAIX, which is highly expressed in parietal cells, colocalized with AE2 in human gastric mucosa, and GST pull-down assays determined that the catalytic domain of CAIX mediated interaction with AE2 (79). Coexpression of CAIX with AE2 increased transport activity by 27 ± 7%, and that of AE1 and AE3 by 32 ± 10% and 37 ± 9%, respectively (79).

In a similar manner, a physical association between AE3 and CAXIV was discovered in the central nervous system (26). Using mouse brain and retinal lysates, CAXIV immunoprecipitated with anti-AE3 antibody, and both AE3 isoforms immunoprecipitated with anti-CAXIV antibody (26). Also, confocal microscopy revealed colocalization of CAXIV with AE3 in Müller and horizontal cells in mouse retina (26). Coexpression of CAXIV and AE3 in HEK293 cells increased the transport activity of AE3 by 120% - this increase was inhibited by the CA inhibitor acetazolamide (26).

These experiments demonstrate that physical interactions with carbonic anhydrases enhance the transport activities of anion exchangers, and further supports the existence of a bicarbonate transport metabolon (Fig 1.2).

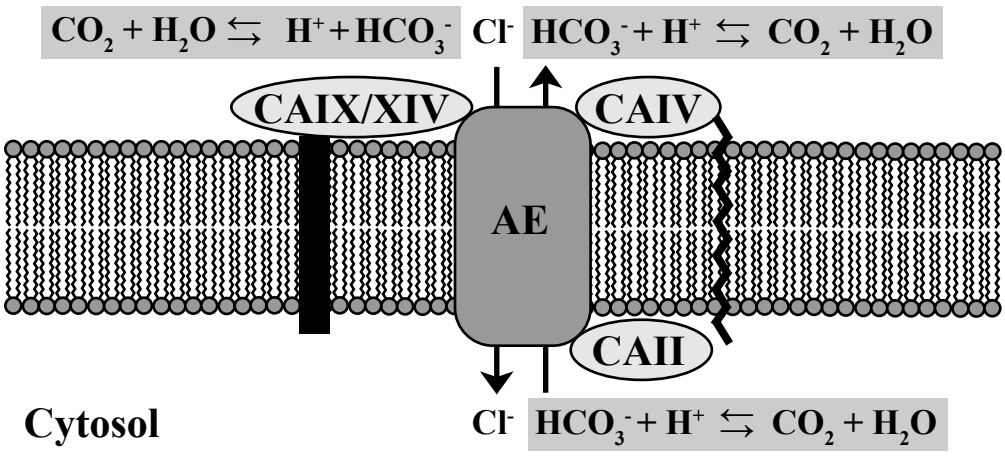

Figure 1.2. The Bicarbonate Transport Metabolon
Cytosolic CAII binds to anion exchangers and provides substrate to the AE active site through the catalysis of CO_2 hydration (136, 137, 138). Extracellular CA isozymes (CAIV, CAIX, and/or CAXIV) are anchored to the plasma membrane via a glycosylphosphatidyl inositol linkage or a transmembrane segment. They bind to anion exchangers and catalyze the reverse reaction, forming CO_2 and H_2O from HCO_3^- and H^+ (26, 79, 122). This allows for efficient HCO_3^- transport, and maintains a HCO_3^- gradient, thereby sustaining AE activity (124).

1.3.3 Other Transporter/Carbonic Anhydrase Interactions

The physical and functional interactions between the SLC4 family of Cl^-/HCO_3^- exchangers and carbonic anhydrases have been well studied. This led to the investigation of CA interactions with other bicarbonate transporters, including members of the SLC26 family and the SLC4 Na^+-coupled HCO_3^- transporters. MCTs have also been shown to physically and functionally interact with CAs. NHE and CA interactions will be discussed in a later section.

The first SLC26 family member found to have a CA binding site, and therefore bind CAII, was SLC26A6 (6). A GST-fusion protein of the Q497-D633 amino acid region of the C terminus of SLC26A6 was blotted onto a membrane, and was able to bind 28 times more CAII lysate than GST alone (6). GSTA6-Q497-D633 also showed saturable binding to CAII in a solid-phase binding assay, while GST alone bound nonspecifically (6). The CAII binding site was further narrowed down to D546-F549 using a series of GST fusion proteins from the Q497-D633 region (6). HEK293 cells transfected with SLC26A6 exhibited a decrease in transport activity with the addition of the CAII inhibitor, ACTZ (6). Both over-expression of CAII-V143Y and mutation of the CAII binding site also reduced the transport activity of SLC26A6 (6). These data indicate that the binding of CAII to SLC26A6 is required for maximal transport activity (5).

SLC26A3 (downregulated in adenoma, or DRA) is one of the only bicarbonate transporters without a CAII binding motif (a hydrophobic residue followed by four amino acids, two are which are acidic e.g. LDADD) (123). This explains why a GST-fusion protein of the C terminal tail of DRA only weakly bound to CAII in comparison to AE1 (123). In HEK293 cells, DRA transport activity required the presence of cytosolic CAII, but was not affected by coexpression with CAII-V143Y (123). While this suggests that a direct physical association with CAII is not required for maximal transport activity of DRA, this is accounted for by the fact that DRA does not bind CAII (123).

A physical and functional interaction between NBCs and carbonic anhydrases was investigated, since carbonic anhydrases catalyze the production of

HCO_3^-, a substrate of NBC, and both proteins are widely expressed in a number of tissues. Coexpression of NBC1 and CAIV in HEK293 cells increased the functional activity of NBC1, and GST pull-down and overlay assays suggested a physical interaction between the two proteins (2). The increase in transport activity was abolished when CAIV was co-expressed with a G767T-NBC1 EC4 mutant, which specified that CAIV binds to the fourth extracellular loop of NBC1 (2). Interactions were also discovered between CAII and NBC1 and NBC3 (67, 101), in that coexpression of CAII with either NBC increased transport activity, and the presence of CAII-V143Y attenuated this effect by 40 ± 7% and 31 ±. 3%, respectively (67). The D1135-D1136 region of NBC3 was determined to be important in the binding of CAII, and mutating this region resulted in the retention of only 29 ± 22% of wild type activity (67). Coexpression of NBC1 and CAII in oocytes increased NBC1 activity compared to NBC1 alone, and this effect was reversed by ETZ or the presence of CAII-V143Y (12). All of these experiments support the existence of a transport metabolon between NBCs and carbonic anhydrases.

An interaction between carbonic anhydrases and MCTs was first observed in oocytes injected with CAII and MCT1. CAII increased the rate of H^+ flux mediated by MCT1, and this increase was independent of added Cl^-/HCO_3^- and was unaffected by the presence of ETZ (14). In another set of experiments, coexpression of MCT1 and the catalytically inactive CAII mutant V124Y increased MCT1 activity to the same degree as wild type CAII (13). Coexpression of MCT1 and CAI or CAII with a mutation in the motif required for binding to AE1, did not induce any increase in MCT1 activity (13). Similar experiments were repeated with MCT4 and CAII, and MCT2 and CAIV, with the same results (15, 56). This suggests that the physical binding of CAII, not the catalytic activity, is the factor affecting MCT1 activity (14). It was also suggested that CAII promotes the dissipation of H^+ from the face of MCT1, preventing the formation of a pH microdomain and maintaining a H^+ gradient (13). This hypothesis was tested by expressing MCT1 or MCT4 with CAII containing a mutation in His64 (CAII-H64A), an important amino acid in intramolecular H^+ shuttling. The CAII-

induced increase in MCT activity previously observed was abolished by CAII-H64A, but was able to be restored by the addition of the H^+ acceptor/donor 4-MI (16).

1.3.4 Bicarbonate Transport Metabolon Controversies

While there has been extensive research regarding physical and functional interactions between carbonic anhydrases and several membrane transporters, there is some controversy regarding the proposed CAII-binding site on the C-terminus of these transporters. One study replicated the solid phase binding assays where SLC4-GST-Ct fusion proteins bound to immobilized CAII, but when they attempted the same experiment with pure SLC4-Ct peptides, no binding was detected (99). They also found that when the SLC4-GST-Ct peptides were immobilized, more CAII bound to just GST than the fusion proteins, and pure SLC4-Ct peptides didn't bind at all (99). Rapid binding of acetazolamide to CAII was detected using surface plasmon resonance, but no binding of CAII to immobilized SLC4-Ct was detected again (99). It was also pointed out that there are members of the SLC4 family that transport HCO_3^- but don't contain the LXXXX binding motif, and members that have the motif but don't transport HCO_3^-, suggesting that while this particular motif might play an important role, it might not be the binding of CAII (20). In defense of the previous studies, it was proposed that SLC4-Ct on its own is not in a structural position to bind to CAII without fusion to a GST protein. Also GST, like AE1, is expressed as a dimer, and therefore it has two points of attachment to participate in interactions with CAII (20).

In another study, NBCe1-A was co-expressed with CAII in oocytes, and the rate of the fall in intracellular pH in the presence of 5% CO_2 was measured, compared to NBCe1-A expressed alone (70). NBCe1-A activity was found to be unaffected by the presence of CAII (70). They also created a fusion protein with enhanced green fluorescent protein (EGFP) fused to the N-terminus of NBCe1-A, as well as to the C-terminus of CAII close to the LXXXX motif (70). The slope conductance of the EGFP-e1-CAII protein was no different from EGFP-e1,

therefore it was concluded that CAII does not enhance the activity of NBCe1-A (70). Another group repeated this study, and found the exact opposite, that NBCe1-A activity was enhanced with increasing amounts of CAII (12). They suggested that the 25 ng of NBCe1-A RNA injected by the first group, versus the 14 ng injected by themselves, may have contributed to an increase in the membrane conductance of the oocytes in their experiments (12). Also, the first group injected 300 ng of CAII, while 50 ng had been sufficient to obtain a half maximal increase in NBCe1-A activity (12). Digital versus manual manipulation of the voltage during the experiments could also account for the differences in the results of the two studies (20). Finally, NBCe1-A activity in the EGFP-e1-CAII fusion protein experiments may have been influenced by the fusion of such a large protein to its N-terminus. GFP is a 26.9 kDa protein, while CAII is 29 kDa, so it is possible that EGFP, being large and close to the active site of NBCe1-A, interfered with the transport of substrate.

1.4 Cardiomyocyte Hypertrophy

Cardiovascular diseases (CVDs) are the leading cause of death globally. In Canada, 29% of mortalities can be attributed to CVDs, and even if successfully treated, the heart damage induced by these diseases often leads to heart failure (109). Heart failure is prevalent in 1% of Canadians over the age of 65 (109), and is generally preceded by cardiac hypertrophy. Pathological cardiac hypertrophy is an adaptive response to the damage caused by CVDs such as hypertension, ischaemia, or myocardial infarction. Concentric hypertrophy is the result of pressure-overload in the heart, and is characterized by reduced left ventricular volume and increased wall thickness, while eccentric hypertrophy is due to volume overload and causes ventricular dilation and wall thinning (11). The increases in myocyte size and protein synthesis associated with hypertrophy are accompanied by increases in fibrosis, arrhythmias, and sarcomere organization (106). This section will focus on the major hypertrophic signaling pathways in

cardiomyocytes (Fig. 1.3), and the contribution of cardiovascular pH regulation in these pathways.

1.4.1 Ca^{2+} Signaling

An increase in cytosolic Ca^{2+} is frequently implicated in the promotion of cardiomyocyte hypertrophy as a result of its activation of several signaling pathways. Increases in cytosolic Ca^{2+} also occur during excitation-contraction coupling, and one hypothesis as to how the cell differentiates between these increases is the presence of Ca^{2+} microdomains around plasma membrane Ca^{2+} transporters (24). Microdomains would allow for localized signaling effects of Ca^{2+} increases, and prevent interference with cardiomyocyte contraction.

β-adrenergic agonists, such as adrenaline, noradrenaline, and isoproterenol, bind to G-protein coupled receptors (GPCR) in the myocyte plasma membrane, which couple to mainly G_s proteins (11). G_s activates adenylyl cyclase, which accumulates cyclic adenosine monophosphate (cAMP) and activates protein kinase A (PKA) (11). PKA is responsible for the phosphorylation of L-type Ca^{2+} channels, ryanodine receptors, phospholamban, and tropinin, all of which play roles in increasing intracellular Ca^{2+} and cardiac contraction (11). Phospholamban binds to and inhibits sarco-endoplasmic reticulum Ca^{2+}-ATPase (SERCA), which transports Ca^{2+} from the cytosol into the sarcoplasmic reticulum. SERCA expression is reduced in hypertrophy and heart failure, and deletion of a single SERCA allele induces hypertrophy and fibrosis in mice experiencing pressure overload from aortic constriction (11). Inhibition of phospholambin blocks hypertrophy, but loss of a functional phospholamban allele induces dilated cardiomyopathy (11). Over-expression of β-adrenergic receptors, G_s, or PKA also results in cardiomyocyte hypertrophy and fibrosis (37). The use of β-blockers to treat heart failure has been shown to prevent the risk of death by 30%, and are associated with reduced expression of the fetal gene program and increased SERCA expression (11).

Phenylephrine (PE) and endothelin-I (ET-1) are examples of α-adrenergic agonists that, along with Angiotensin II (ANGII), bind to GPCRs in myocytes,

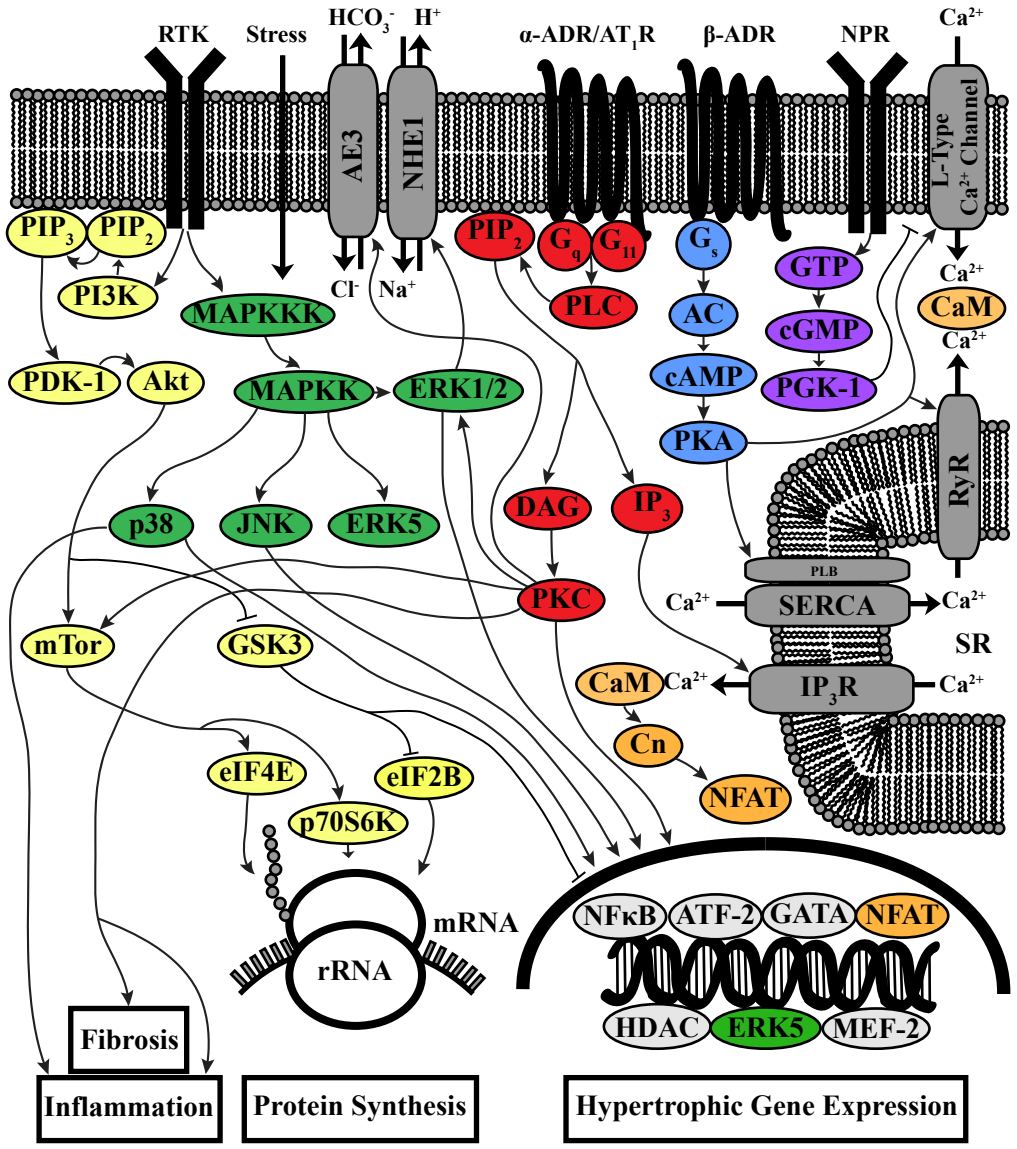

Figure 1.3. Overview of Cardiomyocyte Hypertrophy Signaling Pathways
A summary of some of the interactions in myocytes which promote cardiomyocyte hypertrophy. α-adrenergic, β-adrenergic, and angiotensin II signaling increase cytosolic Ca^{2+}, which activates the calcineurin/NFAT pathway and promotes hypertrophic gene expression (11, 37). Natriuretic peptide signaling inhibits L-type Ca^{2+} channels, thereby inhibiting the calcineurin/NFAT pathway (11). The PI3K/Akt pathway promotes hypertrophy through increases in protein synthesis (106). Activation of the MAPK cascade in turn activates NHE1, as well as induces increases in hypertrophic gene expression and inflammation (108). α-adrenergic signaling also activates PKC, which has a number of downstream targets, including ERK1/2, AE3, and mTor (3, 89). PKC also induces increases in hypertrophic gene expression, fibrosis, and inflammation, all of which promote cardiomyocyte hypertrophy (89).

and activate the G proteins G_q and G_{11} (11). A G_q/G_{11} complex activates phospholipase C (PLC), which induces the hydrolysis of phosphatidylinositol 4,5 biphosphate (PIP_2) producing inositol 1,4,5-triphosphate (IP_3) and diacyl glycerol (DAG) (106). IP_3 binds to receptors on the sarcoplasmic reticulum, inducing the release of Ca^{2+}, increasing cytosolic Ca^{2+} levels (106). Over-expression of G_q and G_{11} is sufficient to induce hypertrophy, while over-expression of a dominant-negative G_q attenuates pressure overload-induced hypertrophy (37). Increased ANGII expression also induces hypertrophy, therefore angiotensin-converting enzyme (ACE) inhibitors have been successful in reducing the risk of death in heart failure (11).

In the hypertrophic signaling pathway, Ca^{2+} binds to calmodulin, a dumbbell-shaped protein with two pairs of Ca^{2+} binding sites separated by an α-helix (71). Upon increases in cytosolic Ca^{2+}, the Ca^{2+} binding sites of calmodulin are occupied, activating the protein so that it is able to recognize and bind to target proteins (71). There are several downstream effects of increases in Ca^{2+} concentration and its subsequent binding to calmodulin, some of which will be discussed in this chapter.

1.4.2 Calcineurin/NFAT Signaling Pathway

The calcineurin/NFAT signaling pathway is one of the most extensively studied portions of the hypertrophic pathway. Calcineurin is a widely expressed serine-threonine phosphatase, made up of a catalytic A subunit, and a regulatory B subunit (37). It has a high affinity for calmodulin ($K_d \sim 1$ nM), which binds to a calmodulin binding domain in the A subunit and displaces an autoinhibitory domain, rendering calcineurin active (55). Activated calcineurin dephosphorylates transcription factors of the nuclear factor of activated T-cells (NFAT) family, revealing nuclear localization signals (37). Upon translocation to the nucleus, NFAT proteins interact with the cardiac-restricted zinc finger transcription factor GATA-4.

GATA-4 is one of six GATA proteins that regulate differentiation, growth and survival of a variety of cell types (100). It is one of the earliest transcription

factors expressed in the fetal heart, and plays an important role in cardiomyocyte differentiation (100). GATA-4 is also expressed in the adult heart, where its zinc fingers bind to the nucleotide sequence element 5'-(A/T)GATA(A/G)-3' of target gene promoters (100). Numerous genes are induced by GATA-4 DNA binding activity, including: myosin heavy chains, natriuretic peptides, and the Na^+/Ca^{2+} exchanger (NCX) (100). Over-expression of GATA-4 activates hypertrophy in cultured neonatal rat cardiomyocytes, and depletion of GATA-4 inhibits PE or ET-1 induced hypertrophy (100).

Calcineurin inhibitors have been used to attempt to inhibit hypertrophy, with varying degrees of success. A number of studies which used the calcineurin inhibitors Cyclosporine A and FK506 found conflicting results, in that some reported an attenuation of PE and ET-1 induced hypertrophy *in vivo*, while others failed to report this effect (37). Over-expression of endogenous calcineurin inhibitors, such as AKAP79 and Cabin/Cain, inhibited increases in calcineurin activity and attenuated hypertrophy *in vitro* and *in vivo* (37). Also, members of the myocyte enriched calcineurin protein family were shown to bind and inhibit the catalytic subunit A of calcineurin (135). While over-expression of calcineurin or NFAT is sufficient to induce hypertrophy, over-expression of a catalytically inactive calcineurin molecule acts in a dominant negative fashion and protects against hypertrophy *in vivo* (37).

1.4.3 Phosphoinositide 3-Kinase and Akt Pathway

Receptor tyrosine kinases (RTK) in cardiomyocytes bind a variety of growth factors, insulin and insulin growth factor (IGF)-1 for example, which in turn activate the signaling enzyme phosphoinositide 3-kinase (PI3K) (106). PI3K is translocated to the membrane, where it phosphorylates the membrane phospholipid PIP_2 to produce phosphatidylinositol 3,4,5 triphosphate (PIP_3) (106). This prompts the translocation of Akt (also known as protein kinase B) and its activator 3-phosphoinositide dependent kinase-1 (PDK-1) to the plasma membrane (106). PDK-1 phosphorylates and activates Akt, which has two main

downstream phosphorylation targets: the mammalian target of rapamycin (mTor) (106) and glycogen synthase kinase 3 (GSK3).

The activation of mTor by Akt results in the phosphorylation of the translational regulator eukaryotic initiation factor 4E (eIF4E), promoting increases in the rate of protein synthesis (88). mTor also phosphorylates and activates p70S6K, which is a short isoform of a ribosomal S6 kinase that plays a role in protein translation (88). In its active, dephosphorylated state, GSK3β prevents hypertrophy through the phosphorylation, and therefore inactivation, of various transcription factors, such as NFAT, GATA-4, etc (88, 125). GSK3β also phosphorylates the translational regulator eIF2B, therefore possibly preventing increases in the rate of protein synthesis (125). Deactivation of GSK3β is not reliant on Akt activity, since it also occurs as a result of GPCR activation, which suggests that GSK3 deactivation might play an important role in the promotion of hypertrophy.

Numerous studies have experimented with this pathway to elucidate the importance of the various kinases. The specific inhibition of PI3K subgroup Iα in transgenic mice prevented physiological hypertrophy as a result of exercise, but the mice were still susceptible to pathological hypertrophy caused by hypertension (37, 106). Over-expression of an activated form of PI3K in transgenic mice was sufficient to induce hypertrophy (37). Short-term over-expression of Akt resulted in physiological hypertrophy and preserved contractility, while long term over-expression generated cardiac dysfunction (106). Over-expression of a phosphorylation-resistant GSK3β in transgenic mice attenuated ET-1 and isoproterenol-induced hypertrophy *in vitro* and *in vivo* (37). While these are just a few of the studies looking at this pathway, the overall relevance of these kinases in respect to hypertrophy is apparent, particularly in the case of GSK3β.

1.4.4 Mitogen Activated Protein Kinase Cascade

Another pathway implicated in the promotion of hypertrophy is the mitogen activated protein kinase (MAPK) cascade. The MAPKs consist of four

subfamilies: extracellular signal-regulated kinases (ERK1/2), c-Jun NH_2-terminal kinases (JNK), p38 kinase, and big MAPK (ERK5) (108). The MAPK of each subfamily is activated by a three-tiered kinase cascade, where a MAPK kinase kinase (MAPKKK) activates a MAPK kinase (MAPKK), which then phosphorylates the MAPK (108). The ERK1/2 pathway is mainly stimulated by growth factors, such as RTKs, but there is also cross talk with GPCRs (108). On the other hand, JNK and p38 are activated by physical, chemical, or physiological stressors, and therefore known as stress-activated MAPKs (SAPKs) (108). All of the MAPKs exert their effects on a variety of protein kinases and transcription factors in the cytosol and the nucleus. This section will attempt to summarize the MAPK pathways and their role in cardiomyocyte hypertrophy.

The phosphorylation of ERK1/2 is downstream of the activation of several other proteins. Growth factors, such as fibroblast growth factor, bind to their respective RTK, which activates Ras (108). Ras translocates Raf to the membrane and activates it, which in turn phosphorylates MEK1/2 (108). MEK1/2 activates ERK1/2, which phosphorylates target proteins, such as transcription factors in the nucleus (108). ERK1/2 also contributes to the regulation of Ca^{2+} channels, potassium channels, and NHE1 in cardiomyocytes (108). Over-expression of Ras in transgenic mice induced cardiomyocyte hypertrophy and induction of the fetal gene program (46). MEK1 over-expression induces hypertrophy *in vitro* and *in vivo* (21), and expression of a dominant negative MEK1 attenuates hypertrophy (132). Expression of a dominant negative Raf attenuates hypertrophy as well (42). Unfortunately, inactivation of the members of the ERK1/2 pathway is also associated with cell apoptosis, suggesting that while this pathway is prohypertrophic, it is also prosurvival (108).

In the JNK pathway, cellular stresses activate MEKKs as well as mixed lineage kinases (MLK2 and MLK3), which in turn activate MKK4 and MKK7 (108). MKK4/7 phosphorylate JNK, which is able to regulate a number of cytoplasmic and nuclear proteins (108). The role of JNK in hypertrophy is not very clear, since there are conflicting results between many *in vitro* and *in vivo* studies. For example, over-expression of a constitutively active MKK7 induce

hypertrophy *in vitro* (141), and the presence of a dominant negative MKK4 attenuated ET-1-induced hypertrophy (27). On the other hand, over-expression of a dominant negative JNK resulted in hypertrophy (63), as well as the cardiac-specific deletion of MKK4 in transgenic mice (66). *JNK*$^{-/-}$ mice were protected from ischemia-reperfusion-induced cell death (48), but they weren't protected from hypertrophy (129). The JNK pathway has been implicated in interfering with the phosphorylation of NFAT (63), which would suggest that this pathway is antihypertrophic, but based on the numerous studies with conflicting results, it is difficult to draw any definite conclusions.

p38, like JNK, is a SAPK, activated by the MKK3 and 6, which are in turn activated by MEKK1-4, TAK1, and ASK1 (108). It is best known for its role in promoting the expression of proinflammatory cytokines (interleukin (IL)-1β, IL-6, and tumour necrosis factor (TNF)-α), although it also directly phosphorylates activating transcription factor (ATF)-2 and myocyte enhancer factor-2 (MEF-2), which regulate hypertrophic gene expression (106). Like JNK, its role in hypertrophy is not well understood, with many conflicting studies. Increased activation of the p38 pathway induced hypertrophy, while inhibition of the pathway attenuated hypertrophy (86). *In vivo*, p38 activation did not induce hypertrophy, but over-expression of MKK3 or MKK6 produced fibrosis and ventricular wall thinning (64). It has been suggested that p38 activity might be more important in cardiac remodelling and contractility, due to its roles in cytokine production, Na^+/Ca^{2+} exchanger transcription, and downregulation of SERCA expression (108).

The ERK5 pathway is activated by both growth factors and stress stimuli, and, rather than activate transcription factors, can function directly as a transcriptional activator (108). ERK5 is phosphorylated by MEK5, which is activated by MEKK2 and MEKK3 (108). Significantly fewer studies have looked at the role of ERK5 in hypertrophy, but the ones that have found that ERK5 activity increases with hypertrophic stimuli, but this activity is decreased once the disease has progressed to heart failure (108). Future studies will further elucidate the role of ERK5 in cardiac pathologies.

1.4.5 Protein Kinase C

Another extensively researched hypertrophic pathway is that which revolves around the serine/threonine kinase protein kinase C (PKC). PKC is a downstream target of α-adrenergic stimulation; it is activated by DAG, which is produced from the hydrolysis of PIP_2 by PLC, as mentioned previously. Human cardiac tissue expresses at least ten isozymes of PKC, but only εPKC and βIIPKC have been associated with hypertrophy (in humans) (33, 89). βIIPKC is upregulated in hypertrophic myocytes, and over-expression in myocytes results in hypertrophy and fibrosis which was attenuated by a βPKC inibitor (33). In contrast, experiments with βPKC knockout mice indicated that βIIPKC is not required for a hypertrophic response (30, 33). Over-expression of εPKC and εPKC activators results in hypertrophy and fibrosis, while εPKC-specific inhibitors decrease fibrosis and prevent cell death (33).

The downstream effects of PKC activation are numerous, and include activation of the previously mentioned mTOR and MAPK enzymes (89). AE3fl is directly phosphorylated by activated PKC (3). The DNA binding activities of several transcription factors are enhanced/inhibited by PKC activation, including GATA-4, ATF-2, NFAT, NFκB, and histone deactylase (HDAC) 5 (33, 89). Tumour growth factor (TGF) β- and matrix metalloproteinase (MMP)-mediated cardiac fibroblast proliferation, migration and adhesion, can be regulated by PKC isozymes (89). PKC also plays a role in the release of cytokines from inflammatory cells like TNF-α and mast cells, which can induce cell damage in cardiac diseases (89). The effect of PKC activation on pH regulatory transmembrane proteins will be discussed in a later section.

1.4.6 The Fetal Gene Program

Cardiac remodeling reintroduces the expression of several genes associated with the development of the fetal heart. This reactivation of the fetal gene program occurs in order to accommodate the mechanical stress and pressure overload associated with hypertrophy. The most common reactivated genes that

have been established as markers of hypertrophy are natriuretic peptides and myosin heavy chains.

1.4.6.1 Natriuretic Peptides

The natriuretic peptides are enzymes highly expressed during embryonic development. They act to regulate blood pressure and body fluid homeostasis through diuresis, natriuresis, and vasodilation (23). They are also implicated in regulating myocyte growth during development, through the suppression of cardiac fibroblast growth (23). There are three types of natriuretic peptides: atrial natriuretic peptide (ANP), brain or B-type natriuretic peptide (BNP), and C-type natriuretic peptide (CNP). ANP is expressed in the atria and hypothalamus, while BNP is expressed in both the atria and the ventricles, and only in the brains of a few species (11). CNP is expressed in the brain, pituitary, vascular endothelium, reproductive tract, bone, and kidneys - very little is expressed in the heart (23).

In the adult heart, very little ANP, BNP, or CNP is expressed, but the levels of all three peptides increase significantly during hypertrophy (11). *Anp*$^{-/-}$ mice were found to have hypertrophy and hypertension under resting conditions, and more extensive hypertrophy than wild type mice under hypertrophic stimulation (32, 81). *Bnp*$^{-/-}$ mice were not hypertrophic, but had increased interstitial fibrosis in the ventricles under resting conditions (130). Knock-out of the CNP gene in mice resulted in dwarfish and early death, both of which were rescued by CNP over-expression in chondrocytes (40).

Both ANP and BNP bind to natriueretic peptide receptor-A (NPR-A), also known as Guanylyl cyclase-A, while CNP binds to NPR-B (11). *Npr-a*$^{-/-}$ mice suffered from hypertension, interstitial fibrosis, and hypertrophy, and over-expressing NPR-A in these null mice and wild type mice reduced both myocyte size and ANP mRNA and protein expression (54, 57). Binding of natriuretic peptides to NPRs induces the conversion of guanosine triphosphate (GTP) to guanosine 3'-5'-cyclic monophosphate (cGMP). The detailed pathway as to how increased cGMP expression affects hypertrophy is unknown, but it is possible that it activates cGMP-dependent protein kinase-1 (PGK-1) (35). PGK-1 inhibits L-

type Ca^{2+} channels, thereby reducing intracellular concentrations of Ca^{2+} and inhibiting the calcineurin/NFAT pathway (35). *Npr-a*$^{-/-}$ mice were also found to have increased NHE1 activity, intracellular alkalinization, intracellular Ca^{2+}, and Akt activity, suggesting that natriuretic peptides prevent hypertrophy by preventing excessive NHE1 activity (53).

1.4.6.2 Myosin Heavy Chains

Myosin is an important protein involved in muscle contraction in the heart. It consists of two heavy chains (MHC), and four light chains (MLC): MHC consists of a long α-helical rod region and a globular head region, where the MLCs are located (82). In ventricular muscle, there are two isoforms of MHC, α-MHC and β-MHC. Both MHC have ATPase activity that allow them to bind and release actin filaments, producing muscle contraction, but α-MHC have a higher ATPase activity than β-MHC, and therefore a faster contraction rate (11). Both isoforms exist in different ratios in different mammalian species; the fast contracting ventricles of mice and rats consist of predominantly α-MHC, while the slow contracting ventricles of humans consist mostly of β-MHC (82).

During human embryonic development, the amount of β-MHC is >95% of total MHC in the ventricles (103). While some literature suggests this amount doesn't decrease significantly in adult ventricles (102), most literature indicate that there is a significant decrease, the ratio of α-MHC:β-MHC being 30:70 (69, 77, 85). During hypertrophy, there is an increase in β-MHC expression, accompanied by a decrease in α-MHC (11). The relative MHC content of the heart doesn't change, but the ratio of α-MHC: β-MHC changes to 5:95 (69, 85). This change is even more pronounced in rodents (11), which have a higher α-MHC:β-MHC ratio, reinforcing an increase in β-MHC mRNA and protein expression as an established marker of hypertrophy.

1.4.7 Role of Acid/ Base Transporters in Cardiomyocyte Hypertrophy

Several cardiovascular pathologies, including ischemia/reperfusion and cardiac hypertrophy, have been attributed to the activity of the electroneutral sodium proton exchanger, NHE1. Cell acidosis, if sustained, will result in reduced binding of Ca^{2+} to troponin C by inactivation of NCX, L-type Ca^{2+} channels, ryanodine receptors, and SERCA (133). NHE1 responds to cell acidosis by expelling protons from the cell in exchange for Na^{+}. Hypertrophic stimulation of PKC leads to phosphorylation of NHE1 by the MAPK pathway, which results in increased transport activity (78). The resulting increase in intracellular Na^{+} promotes hypertrophy through continued activation of PKC (43), as well as through inhibition/reverse action of NCX (96). As discussed, increases in intracellular Ca^{2+} signaling are frequently implicated in the development of hypertrophy. Not only has NHE1 expression been found to be up-regulated under hypertrophic conditions, inhibition of NHE1 prevented the development of hypertrophy both *in vitro* and *in vivo* (31, 49, 59, 144). Despite these promising data, drug trials revealed that NHE1 inhibition did not affect the incidence of myocardial infarction (MI), infarct size, or improve the clinical outcome in patients with a high risk of ischemia or those undergoing reperfusion therapy for acute ST-elevation MI (131, 145).

NHE1 activity has an alkalizing effect, yet there are no major changes in intracellular pH during hypertrophic stimulation (95). This indicates that there is a parallel acidifying pathway in the cardiomyocyte, since otherwise, the alkalosis would auto-inhibit NHE1 activity through a cytosolic modifier site (29). AE3 is the only Cl^{-}/HCO_3^{-} exchanger that is activated through phosphorylation by PKC, which suggests that it is the transporter acting in parallel to NHE1 (3). The acid load provided by AE3 activity sustains NHE1 activity, and thereby promotes hypertrophy.

1.4.8 The Hypertrophic Transport Metabolon

Recent studies have supported the notion of a hypertrophic transport metabolon, that acts to promote cardiomyocyte hypertrophy (25) (Fig. 1.4). As discussed, interactions between AE3 and CAII, in the form of a bicarbonate transport metabolon, have been well established. Along with HCO_3^-, CAII also increases the production of H^+ in the cell, which is substrate for NHEs. Microtiter plate binding assays, affinity blotting, and coimmunoprecipitation experiments demonstrated that the C-terminal region of NHE1 binds CAII in conditions of low pH (62). The H^+ transport rate in cells expressing both CAII and NHE1 was almost 2-fold greater than cells just expressing NHE1, indicating that CAII enhances the activity of NHE1 (62). This was substantiated by a significant decrease in transport activity with the addition of the CAII inhibitor ACTZ, and the inhibition of activity with a catalytically inactive mutant CAII. The binding of CAII to NHE1 allows for the colocalization of H^+ ions to the active site of NHE1, improving proton removal efficiency. The physical interactions between NHE1 and CAII, AE3 and CAII, and the accompanying increase in the transport activities of NHE1 and AE3 when bound to CAII, suggest that these proteins form a transport metabolon. Increases in NHE1 and AE3 transport activities have been implicated in hypertrophy, hence the term hypertrophic transport metabolon.

A recent study revealed that inhibiting CAII in cardiomyocytes, using ETZ, prevents and reverts hypertrophy (4). The increases in cell surface area and ANP mRNA and protein expression, associated with PE-induced hypertrophy in neonatal and adult murine cardiomyocytes were attenuated by 100 μM ETZ. The PE and ANGII-induced increases in the transport activities of NHE1 and AE3, both of which are directly related to hypertrophy, were also attenuated by ETZ. Finally, ETZ prevented PE-induced increases in Ca^{2+} transient frequencies, which indicates that CAII contributes to alterations in Ca^{2+} handling in hypertrophy. These results suggest that CAII plays a role in the hypertrophic cascade, and also support the existence of a hypertrophic transport metabolon.

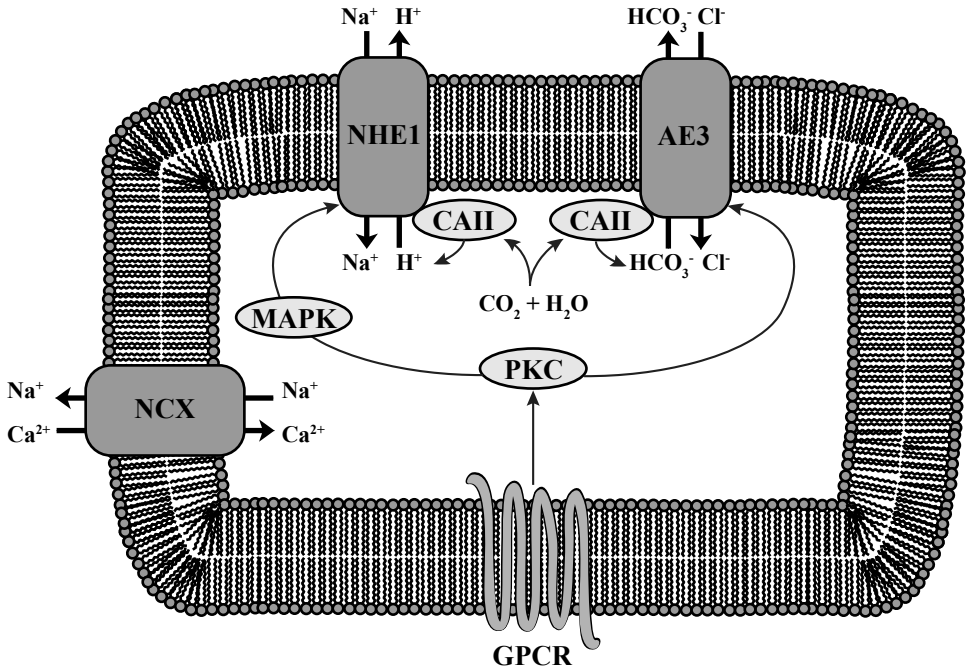

Figure 1.4. The Hypertrophic Transport Metabolon
Hypertrophic agonists, such as phenylephrine and angiotensin II, bind to G-protein coupled receptors (GPCR) on the myocyte plasma membrane (11). This activates PKC, which in turn activates NHE1 through the MAPK pathway (78), and AE3 by direct phosphorylation (3). The acid loading activity of AE3 prevents any NHE1-induced intracellular alkalinzation, thereby preventing any major changes in pH and sustaining the transport activities of both NHE1 and AE3 (3, 97). CAII physically interacts with NHE1 and AE3, thereby providing a continuous, local supply of H^+ and HCO_3^- to the active sites of the transporters (62, 124, 136, 137, 138). Continuous NHE1 activity increases intracellular levels of Na^+, which causes the reverse action/inhibition of NCX (96). An increase in cytosolic Ca^{2+} activates several prohypertrophic pathways in cardiomyocytes.

1.5 Thesis Objectives

The objective of this thesis is to investigate the role of CAII in cardiomyocyte hypertrophy. Previous work revealed that inhibiting CAII prevents and reverts hypertrophy, suggesting that CAII is an important protein in the development of hypertrophy. We explored this further and look at the effect of CAII over-expression, as well as CAII ablation, on hypertrophy *in vitro*.

Experimental materials and methods are described in Chapter 2. Chapter 3 illustrates the use of adenoviral constructs to over-express CAII in neonatal rat ventricular myocytes, and the effect this has on hypertrophic markers. Chapter 4 reports on baseline cardiovascular parameters and cardiac function of *caii*$^{-/-}$ mice compared to wild type mice, and the extent of hypertrophy in these mice. The findings of these studies further support the existence of a hypertrophic transport metabolon, and the importance of CAII in the promotion of cardiomyocyte hypertrophy.

Chapter 2: Materials and Methods

2.1 Materials

Standard lab reagents were purchased from Fisher Scientific (Ontario, Canada), Sigma-Aldrich Canada (Oakville, ON, Canada), and BDH Inc. (Toronto, ON, Canada) and EMD Chemicals (Gibbstown, NJ, USA). All other materials are listed in the following tables.

Table 2.1. **Animals**

Name	**Source**
4-Day-Old Neonatal Rat Pups	Department of Biosciences Animal Service, University of Alberta
C57BL/6 *Car2* Mice	Jackson Laboratories

Table 2.2. **Reagents**

Name	**Source**
2-mercaptoethanol	EMD Chemicals
2,3-butanedione monoxime (BDM)	Sigma-Aldrich
Acetone	Fisher Scientific
Acrylamide	Bio-Rad Laboratories
Ammonium persulfate	Bioshop Canada Inc.
Bovine serum albumin	Sigma-Aldrich
Bromophenol Blue	Sigma-Aldrich
Collagenase B	Roche Applied Science
Collagenase Type 2	Worthington Biochemical Corporation
Complete™ protease inhibitor cocktail tablets	Roche Applied Science
Cytosine β-D-arabinofuranoside (Ara-C)	Sigma-Aldrich
Deoxyribonuclease I	Worthington Biochemical Corporation
dNTP Mix	Fermentas

Dithiothreitol (DTT)	Gibco-Invitrogen Corporation
Dulbecco's Modified Eagle's Medium (DMEM)/Nutrient Mixture F12-Ham	Sigma-Aldrich
ECL chemiluminescent reagent	PerkinElmer
Fetal Bovine Serum	Gibco-Invitrogen Corporation
First-Strand Buffer	Gibco-Invitrogen Corporation
Gentamycin Reagent Solution	Gibco-Invitrogen Corporation
Glycerol	Fisher
HEPES buffer solution	Gibco-Invitrogen Corporation
Horse Serum	Gibco-Invitrogen Corporation
Insulin-Transferrin-Selenium (ITS) Liquid media Supplement 100X	Sigma-Aldrich
L-glutamine	Gibco-Invitrogen Corporation
Mouse Laminin	Gibco-Invitrogen Corporation
N,N,N',N',-tetramethylenediamine (TEMED)	Fisher Scientific
$Oligo(dT)_{18}$	Fermentas
Penicillin	Sigma-Aldrich
Phenylalanine, L-[2,3,4,5,6-^{3}H]-([^{3}H]phenylalanine)	PerkinElmer
Phenylephrine	Sigma-Aldrich
Precision Plus Protein^{TM} Dual Color Standards	Bio Rad Laboratories
Protease type XIV	Roche Applied Science
Restriction Endonucleases	New England BioLabs
RnaseOUT	Gibco-Invitrogen Corporation
Rotor-Gene SYBR Green PCR Master Mix	Qiagen
Sodium-dodecyl sulphate (SDS)	Sigma-Aldrich
Superscript II reverse transcriptase	Gibco-Invitrogen Corporation

Taurine	Sigma-Aldrich
Trichloroacetic acid	BDH Inc.
UltraPure™ Tris	Gibco-Invitrogen Corporation
Trypsin	Worthington Biochemical Corporation
Tween 20	Fisher Scientific

Table 2.3. **Primers**

Name	Sequence
rBNP Fwd	5'-CTTGGGCTGTGACGGGCTGAG-3'
rBNP Rev	5'-GCTGGGGAAAGAAGAGCCGCA-3'
rβ-MHC Fwd	5'-GGCAGAGGAGAGGGCGGACA-3'
rβ-MHC Rev	5'-ACTCTTCATTCAGGCCCTTGGCG-3'
rAE3fl Fwd	5'-ACATGCCTGGGGGAGACGGT-3'
rAE3fl Rev	5'-AGAAAGGCACGCGCCCACA-3'
rNHE1 Fwd	5'-TCAGAGCGCACTTGCCAGCG-3'
rNHE1 Rev	5'-TAGGACCGCAGCCGTTGCC3-'
rGAPDH Fwd	5'-GGCATTGCTCTCAATGACAA-3'
rGAPDH Rev	5'-ATGTAGGCCATGAGGTCCAC-3'
mANP Fwd	5'-TCCAGGCCATATTGGAGCAAATCC-3'
mANP Rev	5'-TCCAGGTGGTCTAGCAGGTTCTTG-3'
mBNP Fwd	5'-TGGGCTGTAACGCACTGAAGTTG-3'
mBNP Rev	5'-TCAAAGGTGGTCCCAGAGCTGGG-3'
mβ-MHC Fwd	5'-GCAGCAGTTGGATGAGGGACT-3'
mβ-MHC Rev	5'-GACTGCCCAGGGCTTGCTCA-3'
mAE3fl Fwd	5'-AGGCTCAAATGTTGGGTTCT-3'
mAE3fl Rev	5'-CTGTATCCGGGATGGTTTCT-3'
mNHE1 Fwd	5'-TTTTCACCGTCTTTGTGCAG-3'
mNHE1 Rev	5'-TGTGTGGATCTCCTCGTTGA-3'
mGAPDH Fwd	5'-CCTCGTCCCGTAGACAAAAT-3'
mGAPDH Rev	5'-TGATGGCAACAATCTCCACT-3'

Table 2.4. **Antibodies**

Name	Source
HRP conjugated sheep anti-mouse IgG	Santa Cruz Biotechnology
HRP conjugated donkey anti-rabbit IgG	Santa Cruz Biotechnology
Mouse anti-β-actin monoclonal antibody	Santa Cruz Biotechnology
HRP conjugated mouse anti-goat IgG	Santa Cruz Biotechnology
Rabbit anti-CAII polyclonal antibody	Santa Cruz Biotechnology
Rabbit anti-GFP polyclonal antibody	Dr. Luc Bertiaume

Table 2.5. **Software**

Name	Source
QCapture Software	Qimaging Corporation
ImagePro Software	Media Cybernetics
Rotor Gene 6.0.14 Software	Qiagen

Table 2.6. **Miscellaneous**

Name	Source
Immobilon-P PVDF membrane	Millipore
Nylon Cell Strainer	Becton Dickinson
Primaria™ tissue culture dishes	Becton Dickinson
Rneasy Plus Mini Kit	Qiagen

2.2 Methods

2.2.1 Animal Care

Experimental protocols involving animals were carried out in accordance with policies of the Canadian Council on Animal Care, and were approved by the Faculty of Medicine and Dentistry, University of Alberta's Animal Care and Use Committee.

2.2.2 Neonatal Rat Cardiomyocyte Isolation and Culture

Neonatal rat cardiomyocytes were isolated and cultured using a protocol based on what has been previously described (58). Hearts were harvested from four day old male rats, following decapitation, and washed 2-3 times in 4 ˚C phosphate-buffered saline (PBS; 140 mM NaCl, 3 mM KCl, 6.5 mM Na_2HPO_4, 1.5 mM KH_2PO_4, pH 7.4). Ventricles were minced and incubated for 20 min at 100 rpm at 37˚C in PBS, containing 2% w/v Collagenase Type 2, 0.5% w/v Deoxyribonuclease I, and 2% w/v Trypsin. After homogenization, 20 ml of DF20 medium (DMEM/Nutrient Mixture F12-Ham, 25% v/v fetal bovine serum, 4 mM L-glutamine, and 0.05 mg/ml Gentamycin Reagent Solution) were added to the myocytes, and the solution was centrifuged for 1 min at 129 x *g*. The supernatant was discarded, being mostly fibroblasts, and the pellet was resuspended in the digestion solution to repeat the homogenization. The supernatants from the three subsequent homogenizations were not discarded, but collected, maintained at 4 ˚C, and centrifuged at 583 x *g* for 7 min. Pellets were resuspended in 10 ml of DF20 medium. The resuspensions were combined, and centrifuged at 583 x *g* for 7 min. The pellet was resuspended in 10 ml of plating medium (DMEM/Nutrient Mixture F12-Ham, 5.9% v/v fetal bovine serum, 12.5% v/v horse serum, 4 mM L-glutamine, and 0.05 mg/ml Gentamycin Reagent Solution), and incubated in a T75 flask at 37 ˚C for 1 h. The supernatant was transferred to another T75 flask, and the first flask washed with 5 ml of plating medium and added to the supernatant. The new flask was incubated for 45 min at 37 ˚C, and then the

supernatant was centrifuged at 202 x *g* for 2 min. The pellet was resuspended in plating medium, and cells were plated at a density of 1.0 x 10^6 cells on 60 mm Primaria™ tissue culture dishes. Dishes were supplemented with 1 μM Cytosine β-D-arabinofuranoside to cause apoptosis in proliferating cells.

2.2.3 Adult Mouse Cardiomyocyte Isolation and Culture

Adult mouse cardiomyocytes were isolated and cultured as previously described (4, 111). Following anesthetization by intraperitoneal injection with sodium pentobarbital (50 mg/kg body mass), hearts were excised and extra-cardiac tissue removed. Retrograde aortic perfusion was performed at a rate of 3 ml/min at 37 ˚C for approximately 3 min with Ca^{2+} free perfusion solution (120 mM NaCl, 5.4 mM KCl, 1.2 mM $MgSO_4$, 1.2 mM NaH_2PO_4, 5.6 mM glucose, 20 mM $NaHCO_3$, 10 mM BDM, and 5mM taurine). The solution was then switched for 15 min to an enzymatic digestion solution (Ca^{2+} free perfusion solution, 0.5 mg/L collagenase B, 50 μM $CaCl_2$, and 0.02 mg/ml protease type XIV). After digestion, the ventricles were removed, cut into several small pieces, and triturated in 2.5 ml of the enzymatic digestion solution using a transfer pipette. An equal amount of myocyte stopping buffer 1 (Ca^{2+} free perfusion solution, 10% (v/v) fetal bovine serum, and 50 μM $CaCl_2$) was added to stop enzymatic digestion, and cells were filtered through a 100 μm nylon cell strainer. The myocytes were allowed to sediment by gravity for 10 min, and the pellet was resuspended in 5 ml of myocyte stopping buffer 2 (Ca^{2+} free perfusion solution, 5% (v/v) fetal bovine serium, and 50 μM $CaCl_2$). Cells were transferred to a 60 mm tissue culture dish, and the Ca^{2+} concentration was increased by adding increasing amounts of $CaCl_2$, incubating for 4 min between each addition. Final concentrations of Ca^{2+} were as follows: 62 μM, 112 μM, 212 μM, 500 μM, and 1 mM. The cells were allowed to sediment by gravity for 10 min, and the pellet was resuspended in plating medium (DMEM/Nutrient Mixture F12-Ham, 5% (v/v) fetal bovine serum, 10 mM BDM, 1 % penicillin, and 2 mM L-glutamine). Myocytes were plated at a density of 0.5-1 x 10^4 cells per 35 mm tissue culture dish. The dishes were precoated for 2 h with 10 μg/ml mouse laminin in PBS.

Cells were incubated for 1 h at 37 ˚C and 5% CO_2, then the medium was replaced with culture medium (DMEM/Nutrient Mixture F12-Ham, 10 mM BDM, 1 % penicillin, 2 mM L-glutamine, 0.1 mg/ml bovine serum albumin, and 1x ITS Liquid Media Supplement).

2.2.4 Generation of Recombinant Adenoviruses

The plasmids pJRC36 (containing the translated and untranslated regions of human CAII) (124) and pDS14 (containing CAII-V143Y) (124) were initially digested with the restriction enzyme, EcoR I. After gel purification, the linearized products were digested using Mung Bean exonuclease to create a blunt end. The final fragments were cloned into the XbaI and EcoRV sites of pAdTRACK-CMV (44). Successful cloning of pDAS1 (containing wild type human CAII) and pDAS2 (containing CAII-V143Y) was confirmed by DNA sequencing (University of Alberta). pDAS1 and pDAS2 were used to generate recombinant adenoviruses by the Cardiovascular Research Centre Gene Transfer Core (University of Alberta). AdCAIIWT encoded for wild type CAII and GFP, and AdCAIIM encoded for mutant CAII and GFP. A recombinant adenovirus encoding only GFP (AdGFP) was also generated to be used as a control.

2.2.5 CAII Deficient Mice

Experiments were performed using male C57BL/6 *Car2* mice. The *caii*$^{-/-}$ mice have a null mutation at the Car-2 locus on chromosome 3, originally achieved by treatment with *N*-ethyl-*N*-nitrosourea (61). Age-matched wild type mice were used as controls.

2.2.6 Heart Weight to Body Weight Ratio

Mice were weighed, then euthanized by intraperitoneal injection with sodium pentobarbital (50 mg/kg body mass). The hearts were excised, rinsed in ice cold PBS. The hearts were excised and rinsed in ice cold PBS. The ventricles

were blotted dry and weighed. Heart weight to body weight ratio was calculated by dividing the weight of the ventricles by the weight of the whole animal.

2.2.7 Blood Pressure and Heart Rate Recordings

Blood pressure and heart rate recordings were collected by the Cardiovascular Research Centre Core Facility (University of Alberta). A warming chamber, restrainers, and tail cuff sensors (IITC Life Science) were used to collect blood pressure measurements (systolic and diastolic) and heart rates from the mice. A chamber temperature of 26 ˚C was used to detect blood pressure pulses in the tail. Three tests (30 s/reading) were performed for each mouse.

2.2.8 Echocardiography

Echocardiography was performed by the Cardiovascular Research Centre Small Animal Echocardiography Core (University of Alberta). Mice were anesthetized using 3.0% Isoflurane in a Vevo Compact Anesthesia System, which was switched to 1.0-1.5% once masks were applied to the animals. Echocardiographic parameters were measured and calculated using a Visualsonics 770 High Resolution Imaging system. Wall measurements, % ejection fraction, and % fractional shortening were calculated, using a 30 MHz probe, to obtain M-mode images in the parasternal long axis and short axis view at the papillary level. Mitral velocities, E and A, were obtained using a 4 chamber view to calculate the mitral valve E/A ratio. The Tissue Doppler was taken from the mitral septal annulus to give the E' tissue motion value, which was used to calculate the E/E' ratio.

2.2.9 Cardiomyocyte Treatment

Neonatal rat ventricular myocytes were incubated for 18 h at 37 ˚C and 5% CO_2, then washed with PBS and wash medium (DMEM/Nutrient Mixture F12-Ham, 4 mM L-glutamine, and 0.05 mg/ml Gentamycin Reagent Solution).

Myocytes were then incubated at 37 ˚C and 5% CO_2 for 48 h in serum-free medium (DMEM/Nutrient Mixture F12-Ham, 1% w/v ITS Liquid Media Supplement 100x, 4 mM L-glutamine, and 0.05 mg/ml Gentamycin Reagent Solution). To transduce the cells, AdGFP, AdCAIIWT or AdCAIIM was added to the appropriate dishes at the same time as the addition of the serum-free medium. 10 μM PE, prepared in water and stored as frozen aliquots, was added 24 h post-transduction.

Adult mouse ventricular myocytes were incubated for 18 h at 37 ˚C and 5% CO_2, then treated with vehicle (control) or 10 μM PE. The cells were incubated in the presence of vehicle or PE for 24 hours at 37 ˚C and 5% CO_2.

2.2.10 Cell Size Analysis

Images of cultured neonatal rat cardiomyocytes were collected 48 h post-transduction, using a QICAM fast cooled 12-bit colour camera (QImaging Corporation). Images of cultured adult mouse cardiomyocytes were collected 24 h after treatment with vehicle or PE. Image-Pro Plus software was used to measure cell surface area. 140-200 cells were measured in each group.

2.2.11 [^{3}H]Phenylalanine Incorporation

[^{3}H]Phenylalanine incorporation assays were performed, using modifications of a protocol previously described (65). [^{3}H]phenylalanine (1 μCi/ml) was added to the cultured myocytes at the time of drug treatment (vehicle or PE), and the cells were incubated for 24 h at 37 ˚C and 5% CO_2. The medium on the dishes was aspirated, and the cells were lysed with 0.5% Triton x-100 and protease inhibitor cocktail and collected in 1.5 ml Eppendorf tubes. 100% Trichloroacetic acid (500 g in 350 ml ddH_2O) was added to the lysates to a final concentration of 40%, and the lysates were incubated at 4 ˚C for 30 min. The lysates were centrifuged for 15 min at 12 682 g, and the supernatants discarded. The pellets were resuspended in 200 μl of 4 ˚C acetone, and centrifuged again for 10 min at 12 682 g. This was repeated twice in total, and the final pellets were

resuspended in 200 µl 0.2 M NaOH, 1% SDS. The radioactivity of [^{3}H]phenylalanine was measured by liquid scintillation counting.

2.2.12 SDS PAGE and Immunoblotting

Neonatal rat cardiomyocytes were plated at a density of 2.0 x 10^6 cells per 60 mm dish. Cells were lysed in sample buffer (20% glycerol, 2% 2-mercaptoethanol, 4% SDS, 0.130 M Tris, bromophenol blue, pH 6.8) and electrophoresed on 12% acrylamide gels. Proteins were transferred to PVDF membranes, blocked with 5% w/v skim milk powder/0.1% Tween/Tris-buffered saline (TBS) (137 mM NaCl, 20 mM Tris, pH 7.4), and incubated overnight at 4 ˚C with the following antibodies: anti-CAII antibody (1:1000), anti GFP antibody (1:30 000), anti-β-actin antibody (1:1000). Immunoblots were washed in TBS/0.1% Tween and incubated with donkey anti-rabbit IgG conjugated to horseradish peroxidase, anti-mouse IgG conjugated to horseradish peroxidase, or mouse anti-goat IgG conjugated to horseradish peroxidase (1:5000). Blots were visualized and quantified using ECL reagent and a Kodak Image Station.

2.2.13 cDNA synthesis

Neonatal rat and adult mouse cardiomyocyte lysates were collected using 350 µl Buffer RLT (Qiagen). RNA was extracted from the lysates using an RNeasy Plus Mini Kit, as per manufacturer's instructions, and quantified using a Nanodrop 2000c spectrophotometer (Thermo Fisher Scientific). RNA (100 ng) was combined with 2 mM dNTP Mix and 25 µg/ml Oligo$(dT)_{18}$, heated to 65 ˚C for 5 min, and chilled on ice for 1 min. First-Strand Buffer, 0.1 M DTT, and 2 units/µl RNaseOUT were added to the mixture, which was then incubated for 2 min at 42 ˚C. SuperScript II reverse transcriptase (200 units) was added (final volume = 20 µl), and the mixture was incubated at 42 ˚C for 1 h, and then 70 °C for 15 min. Three samples were pooled for subsequent analysis.

2.2.14 Quantitative Real-Time PCR

Quantitative real-time PCR (qPCR) was performed in a Rotorgene 3000 (Corbett Research) using 5 µl of template cDNA along with: 12 µl 2x Rotor-Gene SYBR Green PCR Master Mix (Rotor-Gene SYBR Green PCR Kit, Qiagen), and 1 µM of each primer. The program used was: 90 ˚C /5 min - (95 ˚C /5 sec, 60 ˚C /10 sec) 35x. Data were collected with the Rotor Gene 6.0.14 software. Cycle threshold values were collected, in duplicates, for seven transcripts of interest: ANP, BNP, β-MHC, AE3fl, NHE1 and GAPDH. In order to correct for differences in the amount of mRNA between the samples, the cycle threshold values of GAPDH were made to be the same, and that correction was applied to the cycle threshold values of the other proteins. The anti-$\log_2$ of the difference between the cycle threshold values of that of the control represented the relative transcript abundance in the samples compared to the control. The primers were generated using Primer3 (http://frodo.wi.mit.edu/primer3/) – the sequences are indicated in Table 2.3.

2.2.15 Statistics

Data are expressed as mean ± S.E.M. Unpaired *t* tests were used to determine the statistical difference between treatment groups. $P < 0.05$ was considered significant.

Chapter 3: CAII Over-expression and Cardiomyocyte Hypertrophy

The work presented in this chapter utilized adenoviruses that were generated by the University of Alberta Cardiovascular Research Centre Gene Transfer Core. Cloning of pDAS1 and pDAS2 was performed by Daniel Sowah.

3.1 Introduction

The model of a hypertrophic transport metabolon is supported by the physical and functional relationships between CAII, NHE1, and AE3, and the fact that NHE1 inhibition prevents hypertrophy *in vitro* and *in vivo* (62, 124, 136-138). Given that CAII inhibition with ETZ also prevents and reverts cardiomyocyte hypertrophy *in vitro* (4), we wanted to further investigate the importance of CAII in hypertrophy through CAII over-expression in cultured cardiomyocytes.

Physical interactions have been demonstrated between CAII and NHE1, as well as CAII and AE3 (62, 124). The binding of active CAII to these transporters at the plasma membrane creates a continuous local supply of substrate, H^+ and HCO_3^-, enhancing their respective transport activities (62, 124). The acid load created by HCO_3^- extrusion by AE3 is removed by the alkalinizing activity of NHE1, sustaining an intracellular pH of around 7.2 (43). Sustained NHE1 activity produces continuous Na^+ loading of the cell, which results in inhibition/reverse action of the Na^+/Ca^{2+} exchanger (96), and therefore Ca^{2+} loading as well. Increases in cytosolic Ca^{2+}, as discussed, stimulate several hypertrophic pathways.

Since inhibition of CAII with ETZ prevented hypertrophy in cardiomyocytes (4), we hypothesized that over-expression of CAII would also have an effect on hypertrophy. We constructed adenoviruses that encoded wild type CAII and CAII-V143Y, which is a catalytically inactive dominant negative mutant of CAII. Hypertrophic markers were monitored in neonatal rat cardiomyocytes over-expressing each of the respective form of CAII. The essential role of CAII in the hypertrophic transport metabolon suggests that CAII expression is important in promoting and inhibiting cardiomyocyte hypertrophy.

3.2 Results

3.2.1 Adenovirus-mediated CAII over-expression in neonatal rat ventricular myocytes

Unlike other cell types, cardiomyocytes have low transfection efficiency and do not undergo active cell division, which ruled out using transient or stable transfections to over-express CAII. Recombinant adenoviruses have been used to produce high levels of transgene expression in a variety of cell types, without the need for cell division. For the purpose of our experiments, we constructed adenoviruses that encode wild type CAII (AdCAIIWT) or catalytically inactive CAII (AdCAIIM), both of which also encode for GFP. An adenovirus just encoding for GFP was used as a negative control.

To determine how much adenovirus was required to produce an increase in CAII expression, we transduced cultured neonatal rat ventricular myocytes with increasing multiplicities of infection (MOIs) of AdCAIIWT or AdCAIIM. MOI is the ratio of virus particles, or plaque forming units, per cell. Cardiomyocytes were incubated with the adenoviral constructs for 24 h, at which point PE was added to the appropriate dishes. The cardiomyocytes were incubated for another 24 h, for a total of 48 h in the presence of the adenoviruses, and cell lysates were analysed on immunoblots. Increased CAII expression was evident in cardiomyocytes transduced with either AdCAIIWT or AdCAIIM at MOIs of 40, 80, 120, and 160 (Fig. 3.1A). PE treatment induced an even greater increase in CAII expression (Fig. 3.2A).

In order to ascertain an MOI at which the CAII expression between AdCAIIWT and AdCAIIM would be similar, the CAII bands were quantified by densitometry and normalized to levels of β-actin (Fig. 3.1B; Fig. 3.2B). β-actin being a structural protein, its expression is considered to remain consistent between samples, and therefore it is commonly used as a loading control when performing immunoblots. There was no significant difference between the CAII expression of AdCAIIWT and AdCAIIM at each of the MOIs tested. We decided

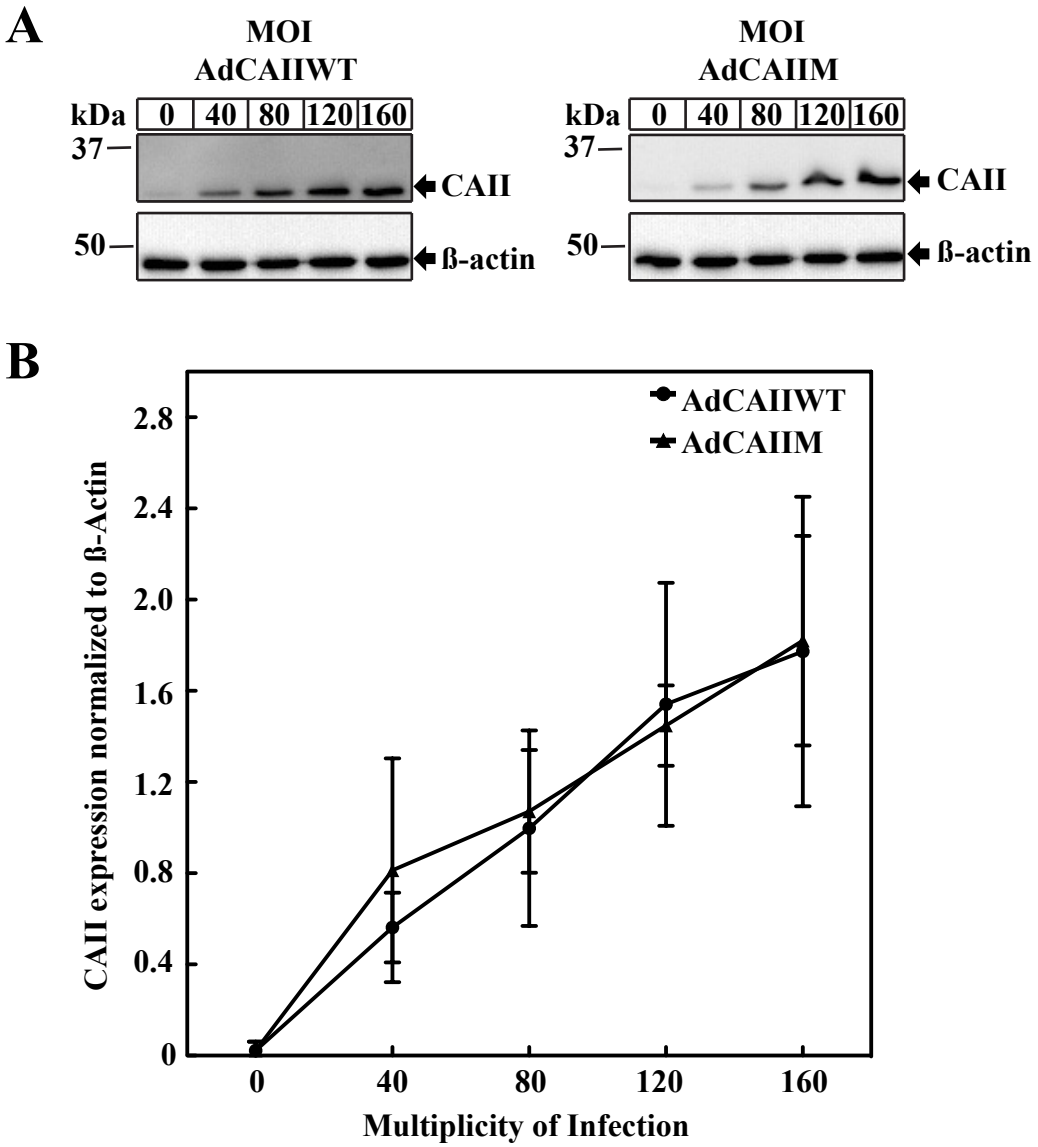

Figure 3.1. Adenovirus-mediated CAII overexpression in neonatal rat ventricular myocytes

Cellular lysates were prepared from neonatal rat ventricular myocytes, which were untreated (0), or transduced with increasing multiplicities of infection (MOI 40, 80, 120, 160) of adenovirus encoding wild type carbonic anhydrase II (AdCAIIWT), or catalytically inactive mutant carbonic anhydrase II (AdCAIIM). *(A)* Immunoblots of the cardiomyocyte lysates were probed with antibodies against CAII and β-actin. *(B)* Expression levels of CAII, normalized to levels of β-actin, were quantified by densitometry. Values are mean ± S.E.M., n = 3.

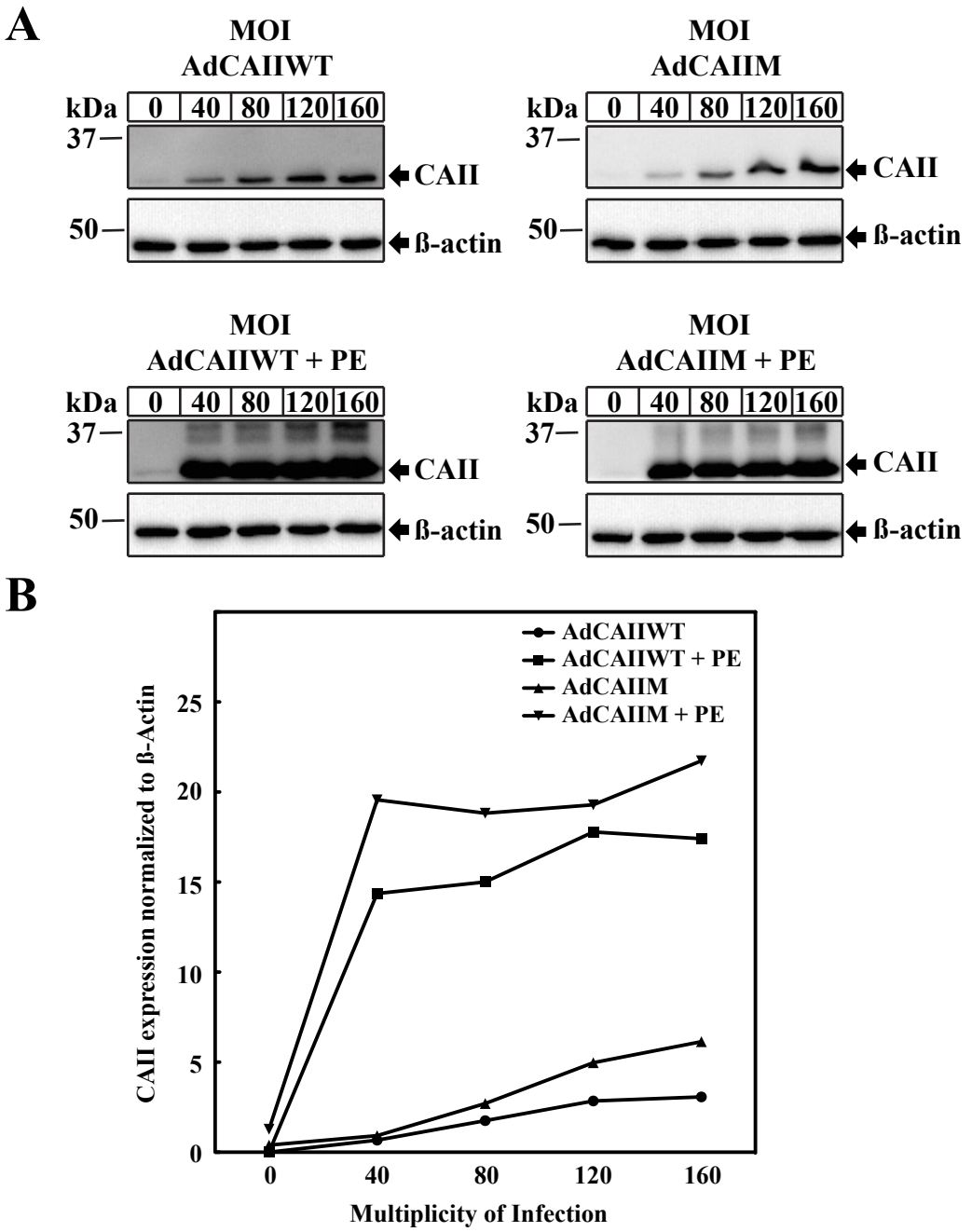

Figure 3.2. Adenovirus-mediated CAII overexpression in neonatal rat ventricular myocytes treated with PE

Cellular lysates were prepared from neonatal rat ventricular myocytes, which were untreated (0), or transduced with increasing multiplicities of infection (MOI 40, 80, 120, 160) of adenovirus encoding wild type carbonic anhydrase II (AdCAIIWT), or catalytically inactive mutant carbonic anhydrase II (AdCAIIM). PE was added to appropriate dishes 24 h post-transduction. *(A)* Immunoblots of the cardiomyocyte lysates were probed with antibodies against CAII and β-actin. *(B)* Expression levels of CAII, normalized to levels of β-actin, were quantified by densitometry; n = 1.

to use an MOI of 80 in subsequent experiments, since CAII is sufficiently over-expressed at this MOI, and there is less chance of side effects from viral overload, that can be caused from using higher viral MOI.

We also had to ensure that the adenoviruses would express the same amount of GFP, in order to be sure that we would be observing the effect of CAII over-expression, not GFP. The same immunoblots used to look at CAII expression were stripped and re-probed with a rabbit polyclonal anti-GFP antibody. Cells transduced with AdGFP at an MOI of 12 were found to express a similar amount of GFP as AdCAIIWT and AdCAIIM at MOIs of 80 (Fig. 3.3). AdGFP at an MOI of 12 was therefore used in subsequent experiments as a control.

3.2.2 Effect of CAII over-expression on cell surface area

The heart increases in size under hypertrophic conditions. Therefore, cell surface area is considered a key marker of hypertrophic growth. In order to determine whether CAII over-expression affects cell surface area, cultured neonatal rat ventricular myocytes were transduced with AdGFP, AdCAIIWT, or AdCAIIM 24 hours after plating, and treated with PE 24 h later. Images of the myocytes were taken 48 h after adenoviral transduction, and cell surface areas were manually measured using ImagePro Plus (Fig. 3.4A).

Over-expression of wild type or catalytically inactive CAII alone did not induce any change in cell surface area compared to control (AdGFP) myocytes (Fig.3.4.B). An increase in cell surface area was evident in control (AdGFP) myocytes and in myocytes over-expressing wild type CAII (AdCAIIWT) treated with PE. Over-expression of CAII-V143Y (AdCAIIM) in the presence of PE did not induce an increase in cell surface area in cardiomyocytes, and the cell surface area was found to not be significantly different from control myocytes (AdGFP).

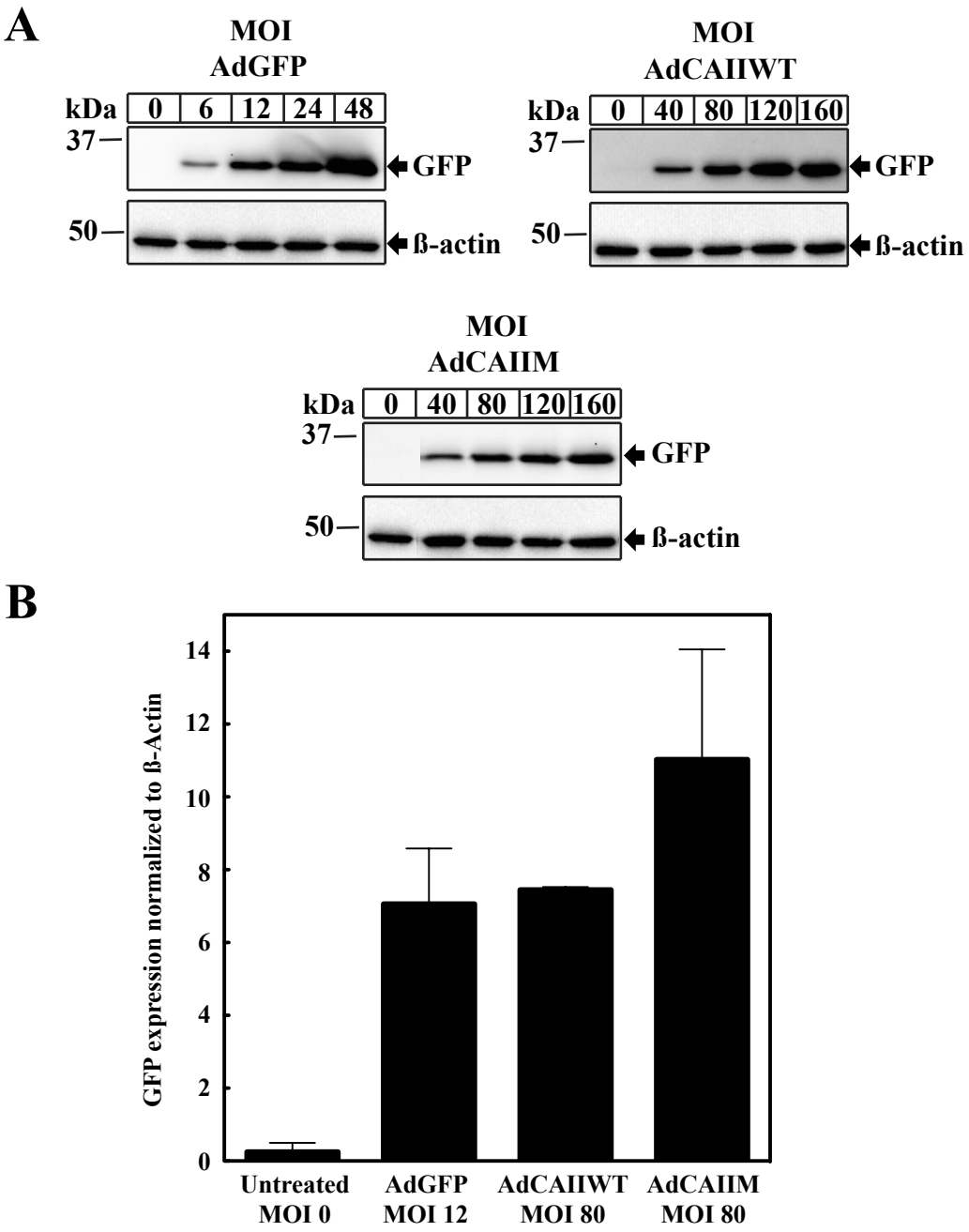

Figure 3.3. Adenovirus-mediated GFP expression in neonatal rat ventricular myocytes

Cellular lysates were prepared from neonatal rat ventricular myocytes, and subsequently transduced with an adenovirus encoding GFP (AdGFP; MOI 12), wild type CAII and GFP (AdCAIIWT; MOI 80) , or catalytically inactive mutant CAII and GFP (AdCAIIM; MOI 80). Untreated myocytes were not transduced with any adenovirus, and therefore represent MOI 0. *(A)* Immunoblots of the cardiomyocyte lysates were probed with antibodies against GFP and β-actin. *(B)* Expression levels of GFP, normalized to levels of β-actin, were quantified by densitometry. Values are mean ± S.E.M., $n \geq 3$.

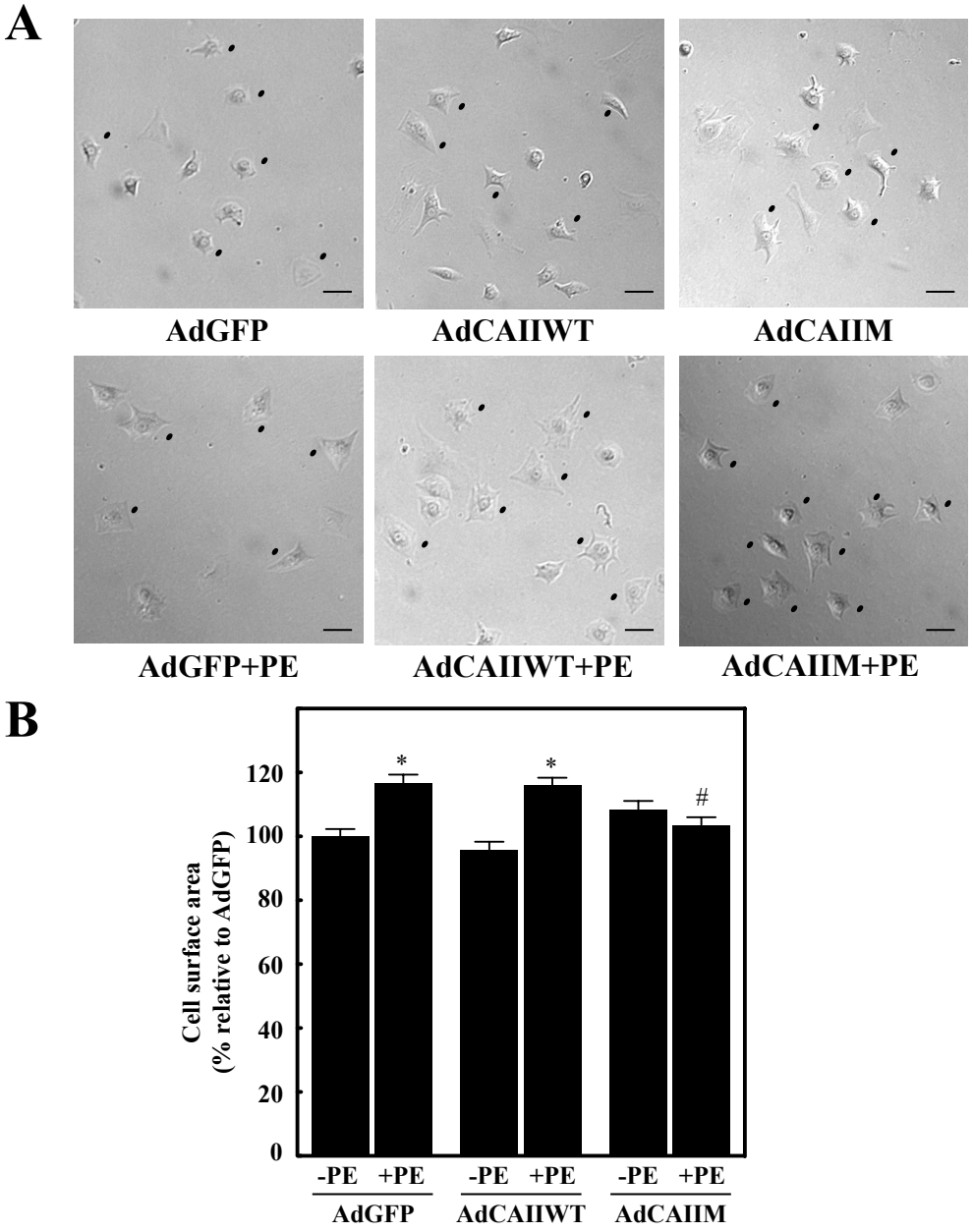

Figure 3.4. Effect of PE on the cell surface area of cultured neonatal rat ventricular myocytes overexpressing wild type or catalytically inactive CAII
(A) Images of cultured rat neonatal myocytes transduced with adenovirus encoding green fluorescent protein (AdGFP), wild type carbonic anhydrase II (AdCAIIWT), or catalytically inactive mutant carbonic anhydrase II (AdCAIIM). Scale bars are 50 µm. Cells were transduced with the respective adenovirus after 18 h of culture, and 24 h later the appropriate cells were treated with 10 µM PE. Cells were imaged 24 h after incubation with PE. Examples of cells used for cell surface area measurement are indicate by a black dot. *(B)* Cell surface areas were measured and displayed as % relative to AdGFP. Values are mean ± S.E.M., n = 4-5 for each group with 120-180 in each group. *P < 0.05, compared with AdGFP. #P < 0.05, compared with AdGFP treated with PE.

3.2.3 Effect of CAII over-expression on protein synthesis

In order to accommodate the growth that is characteristic of cardiomyocyte hypertrophy, the heart increases its protein and RNA content (18). Protein synthesis in cells can be assessed by incubating cells in the presence of aradio-labeled amino acid, and then measuring the radioactivity of the total protein to determine the extent to which the isotope was incorporated. We used this method, incubating cardiomyocytes over-expressing CAII [^{3}H]phenylalanine for 24 h. Proteins were precipitated from cell lysates with trichloroacetic acid, and counted in a liquid scintillation counter.

As with the cell surface data, over-expression of wild type or catalytically inactive CAII alone did not induce any change in protein synthesis compared to control (AdGFP) myocytes (Fig. 3.5). There was a significant increase in protein synthesis in control myocytes and myocytes over-expressing wild type CAII (AdCAIIWT) treated with PE. Protein synthesis in cardiomyocytes over-expressing CAII-V143Y (AdCAIIM) in the presence of PE was not significantly different from control myocytes, indicating that the presence of a catalytically inactive CAII was sufficient to attenuate hypertrophy.

3.2.4 Effect of CAII over-expression on hypertrophic gene expression

Under hypertrophic conditions, the heart is known to reactivate its fetal gene program and upregulate the mRNA and protein expression of a number of genes. Increased mRNA and protein expression of ANP, BNP, and β-MHC are established markers of hypertrophy. RNA was purified from cardiomyocyte lysates over-expressing CAII, and cDNA synthesized using the RNA as template. qPCR allowed for the determination of the PCR cycle at which transcript expression increased exponentially, and therefore gives a relative measure of the amount of transcript present in each sample.

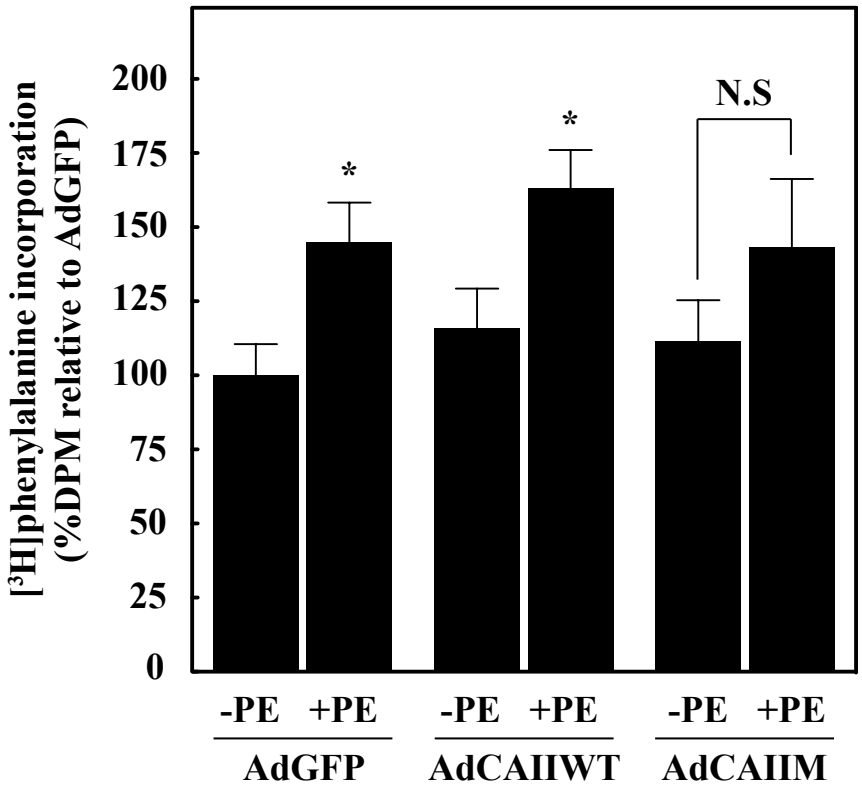

Figure 3.5. Effect of PE on the rate of protein synthesis in cultured neonatal rat ventricular myocytes overexpressing wild type or catalytically inactive CAII

Cultured neonatal rat myocytes were transduced for 24 h with adenovirus encoding green fluorescent protein (AdGFP), wild type carbonic anhydrase II (AdCAIIWT), or catalytically inactive mutant carbonic anhydrase II (AdCAIIM). The appropriate dishes were treated with 10 μM phenylephrine (PE), and all cells were incubated with [^{3}H]phenylalanine (1 μCi/ml). Incorporated [^{3}H] was quantified after 24 h. Values are mean ± S.E.M., n = 4. *P < 0.05, compared with AdGFP not treated with PE. #P < 0.05, compared with AdGFP treated with PE.

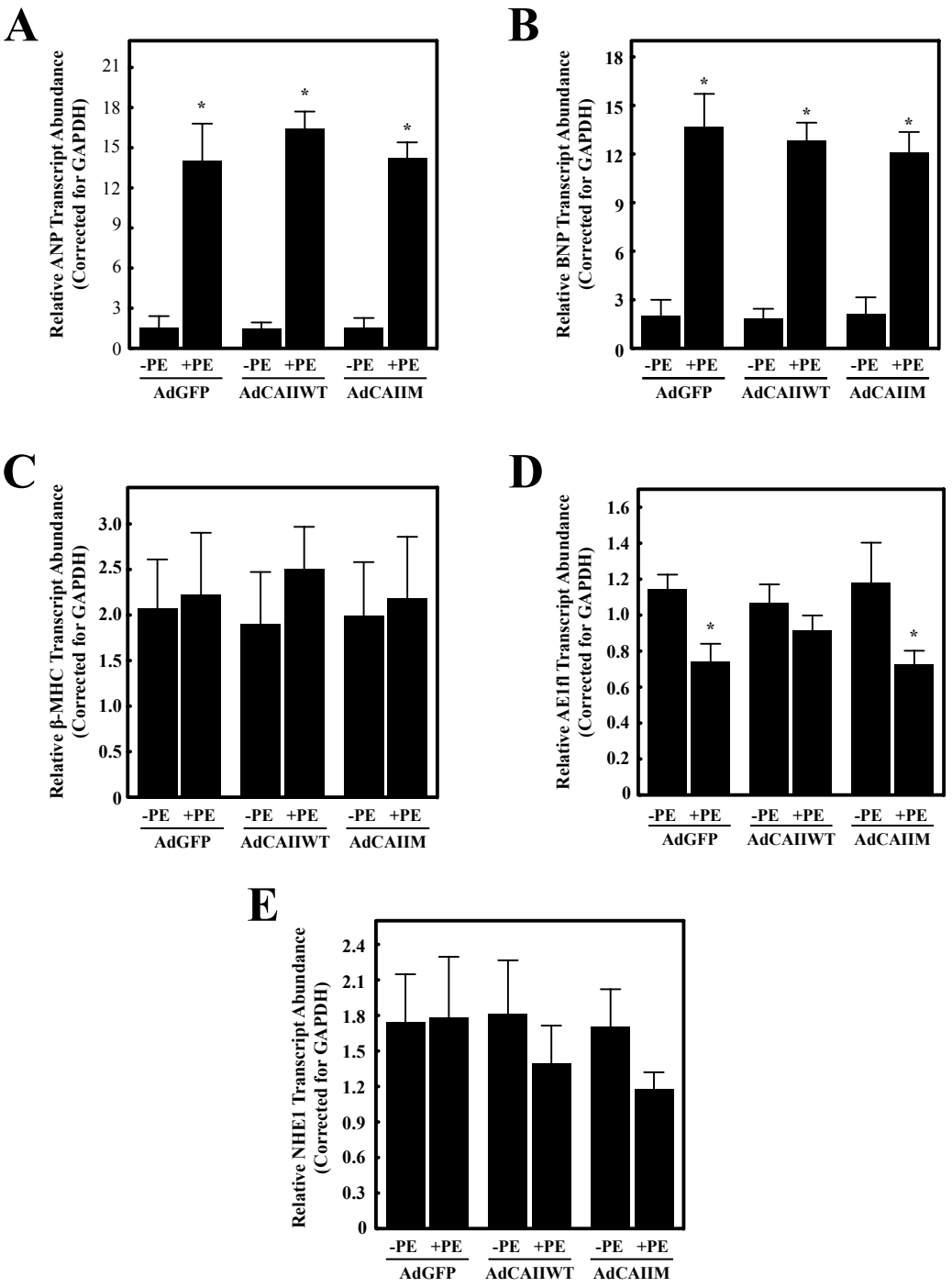

Figure 3.6. Effect of PE on hypertrophic marker and transporter transcript expression in cultured neonatal rat ventricular myocytes overepressing wild type or catalytically inactive CAII

qPCR analysis of *(A)* ANP, *(B)* BNP, *(C)* β-MHC, *(D)* AE3fl, and *(E)* NHE1 mRNA expression in cultured rat neonatal myocytes. Data were corrected for variation using GAPDH expression and results are expressed as transcript expression normalized to GAPDH. Values are mean ± S.E.M., n = 3 for each treatment group. *P < 0.05, compared with AdGFP.

ANP and BNP transcript abundance were not significantly different in cardimyocytes over-expressing wild type or catalytically inactive CAII from control (AdGFP) myocytes (Fig. 3.6A-B). The addition of PE induced a 15-fold increase in the transcript expression of both natriuretic peptides in all three groups, which is generally considered to be indicative of hypertrophy. None of the PE-treated groups were significantly different from one another. Despite being a commonly used marker of hypertrophy, β-MHC expression did not increase in control myocytes treated with PE; all groups, with and without PE, were not significantly different (Fig. 3.6C).

To determine if CAII over-expression has any effect on the other members of the hypertrophic transport metabolon, the transcript abundances of AE3fl and NHE1 were ascertained. Cardiomyocytes over-expressing wild type CAII or CAII-V143Y were not significantly different from control myocytes in terms of AE3fl transcript abundance (Fig. 3.6D). Treatment of control myocytes and myocytes over-expressing CAII-V143Y in the presence of PE induced a significant decrease in AE3fl transcript abundance. This decrease was not observed in PE-treated myocytes over-expressing wild type CAII. NHE1 transcript abundance was not affected by CAII over-expression or the presence of PE (Fig. 3.6E).

3.3 Discussion

Over-expression of wild type CAII had no effect on hypertrophic markers in cardiomyocytes. CAII expression was previously found to increase upon hypertrophic stimulation, which suggested that over-expression of CAII might contribute to hypertrophy. It is possible that NHE1 and AE3 are already saturated with CAII, therefore over-expressing CAII would not increase transport activity or induce hypertrophy. The effect of PE on hypertrophic markers in cardiomyocytes was also not altered by over-expression of wild type CAII, yet there was significantly more CAII expressed in the presence of PE. This is not surprising, considering that PE stimulates protein synthesis in the heart.

Hypertrophic markers were also not affected by over-expression of the catalytically inactive mutant CAII, CAII-V143Y. This mutant acts in a dominant-negative fashion, competing with, and displacing, endogenous CAII bound to NHE1 and AE3, reducing each of their respective transport activities (62, 124). Over-expression of CAII-V143Y in cardiomyocytes in the presence of PE prevented increases in cell surface area and protein synthesis, which suggests that the binding of CAII-V143Y to NHE1 and AE3 is sufficient to attenuate hypertrophy.

Contrary to these results, increases in ANP and BNP transcript abundance in the presence of PE were unaffected by over-expression of CAII-V143Y. One can speculate that the pathway which induces fetal gene reactivation does not overlap with the activity of the hypertrophic transport metabolon. Studies performed with calcineurin Aβ-null mice found that while these mice, were impaired in their ability to produce a hypertrophic response upon stimulation with ANGII, isoproterenol, or pressure overload by aortic banding, mRNA levels of ANP and β-MHC were not reduced (22). The use of rapamycin *in vitro* blocked α-adrenergic agonist-induced increases in cell surface area, while the α-actinin and ANP transcript levels were unaffected (19). Transgenic mice over-expressing both GSK-3β and calcineurin exhibited inhibition of hypertrophy, without reduction in ANP and BNP transcript levels (8). Transgenic mice with a cardiac-specific activated form of MKK7, which is upstream of JNK, exhibited reactivation of the fetal gene program, extracellular matrix remodeling and loss of gap junctions, but no hypertrophy (97). Finally, a dominant-negative PI3K mutation upregulated ANP transcript expression while suppressing cardiac growth *in vivo* (115). These studies reflect on the divergence of the transcriptional and translational pathways in hypertrophy (19), as well as the anti-hypertrophic effects of natriuretic peptides (37). Although upregulation of ANP and BNP is commonly considered a marker of hypertrophy, perhaps they are actually acting in parallel with the protein of interest to attenuate hypertrophy, which suggests that their upregulation could also be a marker of hypertrophic decline.

While a disconnect between reactivation of the fetal gene program and the hypertrophic transport metabolon is an appealing idea, previous experiments showed that 100 μM ETZ was able to partially attenuate PE-induced increases in ANP transcript abundance in neonatal rat cardiomyocytes (4). It is possible that ETZ, being a non-specific CA inhibitor, exerts its inhibitory effects on other CA isozymes in the heart, which might play a more fundamental role in reactivation of the fetal gene program than CAII. It is most likely that natriuretic peptide expression is a more sensitive marker of hypertrophy than cell surface area and protein synthesis. While over-expression of CAII-V143Y is able to attenuate cardiac growth in the time frame of our experiments, natriuretic peptide expression may not respond as rapidly. Since cardiac function is reduced as a result of cardiac growth, not an increase in natriuretic peptide expression, attenuated cardiac growth is a more pertinent indicator of attenuation of hypertrophy.

Reactivation of the β-MHC gene is another established marker of hypertrophy, yet in these experiments it was unaffected by the presence of PE. Recent studies of β-MHC reexpression in the individual myocyte suggest that β-MHC is not a required marker of hypertrophy, since hypertrophy can be induced without β-MHC reexpression (92). For example, experiments with transgenic mice that express β-MHC tagged with a yellow fluorescent protein revealed that β-MHC reexpression occurs mostly in areas of fibrosis within the heart, and that cell size does not determine which cells reexpress β-MHC (91). The conclusion of this study was that β-MHC reexpression might actually be a marker of fibrosis, rather than hypertrophy (91).

Another study used an antibody against β-MHC in cardiomyocytes in a set of flow cytometry and immunohistochemistry experiments (68). They were able to isolate a huge number of myocytes, 10 000-20 000 per heart, using collagenase perfusion, and measure β-MHC reexpression, myocyte size, and tissue distribution (68). Their findings were that β-MHC is only reexpressed in nonhypertrophic myocytes, reexpression occurs in subsets of myocytes throughout the heart, and that levels of α-MHC are consistent between β-MHC

expressing myocytes and myocytes not expressing β-MHC (68). Despite being slightly contradictory amongst themselves, both of these studies challenge previous ideas regarding β-MHC reexpression as a marker of hypertrophy. They also provide some insight into why we may have been unable to see β-MHC reexpression during PE-induced hypertrophy in cardiomyocytes.

CAII physically and functionally interacts with both AE3 and NHE1 in cardiomyocytes, forming a hypertrophic transport metabolon. In over-expressing CAII in cardiomyocytes, we wanted to see if this would affect the expression of the other members of the metabolon. Both AE3fl and NHE1 transcript abundances are unaffected by over-expressing either wild type CAII or CAII-V143Y, except for a significant decrease of AE3fl transcript by 0.2 – 0.5 fold in the presence of PE in control myocytes and myocytes over-expressing CAII-V143Y. This occurs over such a small scale though when compared to the other genes tested, therefore we noted this "significant" decrease, but do not consider it significant enough from which to draw any conclusions.

We suggested that over-expression of wild type CAII does not induce hypertrophy in cardiomyocytes, as indicated by the cell surface area and protein synthesis data, due to saturation of the transport activities of AE3 and NHE1. The fact that the AE3fl and NHE1 transcript abundances are not affected by over-expression of CAII complements this hypothesis. If there had been an increase in AE3 and NHE1 expression, we would have expected an increase in hypertrophic markers due to the increase in Na^+ loading, and in turn Ca^{2+} loading, in the myocytes. Over-expression of a catalytically inactive mutant did not affect cell surface area or protein synthesis either, which suggests that there is also sufficient endogenous CAII present to saturate the transport activities of AE3 and NHE1. Yet, in the presence of PE, over-expression of CAII-V143Y is able to compete with endogenous CAII to a degree that is sufficient to at least partially attenuate a hypertrophic response. This data further supports the existence of a hypertrophic transport metabolon in cardiomyocytes, and the potential of CAII as a therapeutic target in cardiac hypertrophy and heart failure.

Chapter 4: *Caii*$^{-/-}$ Mice and Cardiomyocyte Hypertrophy

4.1 Introduction

The hypertrophic transport metabolon has a place of importance in the promotion and reversion of cardiomyocyte hypertrophy. The focus was originally on NHE1 inhibition, which attenuated hypertrophy *in vitro* and *in vivo* (31, 49, 59, 144). Unfortunately, NHE1 inhibition as an intervention in cardiovascular disease has not come to fruition due to conflicting results in clinical trials using the NHE1 inhibitors cariporide and eniporide (9). The relationship between NHE1 and CAII suggests a role for CAII in cardiomyocyte hypertrophy. This is supported by previous studies demonstrating that the CAII inhibitor ETZ is able to prevent, and revert increases in markers of hypertrophy (4). We wanted to use *caii*$^{-/-}$ mice to further explore the potential of CAII as a pharmacological target in heart failure.

The line of *caii*$^{-/-}$ mice used in our studies was originally generated by chemical-induced random mutagenesis using *N*-ethyl-*N*-nitrosourea (61). The induced-mutation was later determined to be a C-to-T mutation at position 508, producing a premature stop codon at codon 155 (90). This mutation results in decreased CAII mRNA transcript expression, and the absence of CAII protein expression in all tissues (90). *Caii*$^{-/-}$ mice are often runted, and exhibit renal tubular acidosis compared to wild type mice (61).

On the basis of the observation that cardiomyocyte hypertrophy is attenuated by treatment with ETZ, we had reason to believe that *caii*$^{-/-}$ mice would be protected from hypertrophic stimulation. Cardiomyocytes isolated from wild type and *caii*$^{-/-}$ mice from the same colony were monitored for changes in cell surface area, protein synthesis, and hypertrophic gene expression in the presence of vehicle or PE. Nevertheless, since this is not a heart-specific knockout of CAII, our experimental results should be interpreted with some caution.

4.2 Results

4.2.1 Baseline cardiovascular parameters of wild type and *caii*$^{-/-}$ mice

Several cardiovascular parameters of wild type and *caii*$^{-/-}$ mice were measured prior to *in vitro* experiments in order to ascertain any differences between the two lines. Data were collected from 1-3 month old male wild type and *caii*$^{-/-}$ mice. No significant differences in heart weight, body weight, heart rate, and blood pressure were observed between the two strains (Table 4.1). The *caii* $^{-/-}$ mice had a significant increase in heart weight/body weight ratio compared to wild type mice. This increase was the result of both an increase in heart weight (0.16 ± 0.01 g wild types vs 0.19 ± 0.01 g *caii*$^{-/-}$) and a decrease in body weight (31 ± 3 g wild types vs 24 ± 2 g *caii*$^{-/-}$).

4.2.2 Echocardiographic analysis of wild type and *caii*$^{-/-}$ mice

Echocardiographs of wild type and *caii*$^{-/-}$ mice were performed in order to assess their systolic and diastolic cardiac function. Ejection fraction and fractional shortening were both increased in *caii*$^{-/-}$ mice, although not significantly (Table 4.2). *Caii*$^{-/-}$ mice also exhibited, although not significant, an increase in intraventricular septal and left ventricular posterior wall thickness during both systole and diastole, as well as a decreased left ventricular internal diameter. The increase in wall measurements accounts for the increase in left ventricular mass. This data suggests that *caii*$^{-/-}$ mice exhibit increased systolic function.

To assess diastolic function, blood flow velocities through the mitral valve were measured during left ventricular diastole (early filling phase – E wave) and left atrial systole (atrial kick – A wave). A lower E/A ratio would suggest that more blood is entering the ventricle from the atrial kick than during ventricular relaxation, and therefore diastolic dysfunction. Mitral valve tissue motion during

Table 4.1. **Baseline cardiovascular parameters of wild type and *caii*$^{-/-}$ mice**
Hearts were collected from euthanized mice, weighed, and divided by body weight to get the heart weight/body weight ratio. Heart rate, systolic blood pressure, and diastolic blood pressure were obtained using an IITC warming chamber, restrainers and tail cuff sensors. Three tests (30 s/reading) were performed per mouse. Values are expressed as means ± S.E.M. ($n \geq 6$ per group), *$P < 0.05$. HW, heart weight; BW, body weight; HR, heart rate; BPs, systolic blood pressure; BPd, diastolic blood pressure. The HW/BW ratio was significantly different between wild type and *caii*$^{-/-}$ mice.

	WT	*caii* $^{-/-}$
HW, g	0.16 ± 0.01	0.19 ± 0.01
BW, g	31 ± 3	24 ± 2
HW/ BW	0.0054 ± 0.0002	0.0078 ± 0.0003*
HR, bpm	493 ± 30	541 ± 95
BPs , mmHg	131.0 ± 1.5	135.4 ± 4.8
BPd, mmHg	73 ± 4	81 ± 7

Table 4.2. **Echocardiographic analysis of wild type and *caii*$^{-/-}$ mice**
Parameters were measured and calculated using a Visualsonics 770 High Resolution Imaging system. Values are expressed as means ± S.E.M. (n = 6 per group); *P < 0.05. EF, % ejection fraction; FS, % fractional shortening; LVM, left ventricular mass; IVSd, diastolic intraventricular septal wall thickness; LVIDd, diastolic left ventricular internal diameter; LVPWd, diastolic left ventricular poster wall thickness; IVSs, systolic intraventricular septal wall thickness; LVIDs, systolic left ventricular internal diameter; LVPWs, systolic left ventricular posterior wall thickness; MV E/A, ratio of peak E wave mitral valve velocity to peak A wave mitral valve velocity; E/E', ratio of peak E wave mitral valve velocity to E wave mitral valve tissue motion; IVRT, isovolumic relaxation time. The E/E' ratio was significantly different between wild type and *caii*$^{-/-}$ mice.

	WT	*caii* $^{-/-}$
EF, %	53 ± 4	62 ± 4
FS, %	27 ± 3	33 ± 3
LVM	85 ± 7	92 ± 7
IVSd, mm	0.74 ± 0.03	0.82 ± 0.05
LVIDd, mm	4.0 ± 0.1	3.8 ± 0.1
LVPWd, mm	0.73 ± 0.03	0.84 ± 0.05
IVSs, mm	1.0 ± 0.1	1.2 ± 0.1
LVIDs, mm	2.9 ± 0.2	2.6 ± 0.2
LVPWs, mm	1.0 ± 0.1	1.2 ± 0.1
MV E/A ratio	1.6 ± 0.1	1.5 ± 0.1
E/E'	35 ± 4	25 ± 1 *
IVRT, ms	17 ± 1	18 ± 1

the E and A waves was also measured using tissue doppler echocardiography. A lower E/E' ratio is indicative of decreased blood flow into the left ventricle during diastole with increased mitral valve motion, which also implies diastolic dysfunction. The E/A ratio in *caii*$^{-/-}$ mice, although slightly lower, was not significantly different from wild type, but the E/E' ratio of *caii*$^{-/-}$ mice was significantly lower (Table 3.2). Another measure of diastolic function is isovolumic relaxation time (IVRT), which is the time from the closure of the aortic valve to the opening of the mitral valve, and the initiation left ventricular filling. An increased IVRT would reflect prolonged myocardial relaxation, and therefore diastolic dysfunction. Yet the IVRT of *Car2* mice was not significantly different from WT mice; therefore, diastolic dysfunction in these mice is unlikely.

4.2.3 Effect of phenylephrine on cell surface area of cultured cardiomyocytes from *caii*$^{-/-}$ mice

Hypertrophic stimulation induces an increase in cardiomyocyte size in order to accommodate decrease cardiac function. In order to assess whether this occurs in the absence of CAII, adult mouse ventricular myocytes were cultured from wild type and *caii*$^{-/-}$ mice and treated with 10 μM PE or vehicle 18 h after plating. Images of the myocytes were taken 24 h after treatment, and manually measured using ImagePro Plus (Fig. 4.1A).

Cell surface area increased significantly, approximately 20%, with the addition of PE in myocytes cultured from wild type mice, which is comparable to previous studies (4) (Fig. 4.1B). In myocytes cultured from *caii*$^{-/-}$ mice, treatment with PE did not induce any increase in cell surface compared to vehicle-treated myocytes. However, compared to vehicle-treated myocytes from wild type mice, there was an increase cell surface area of both vehicle and PE treated myocytes from the *caii*$^{-/-}$ mice.

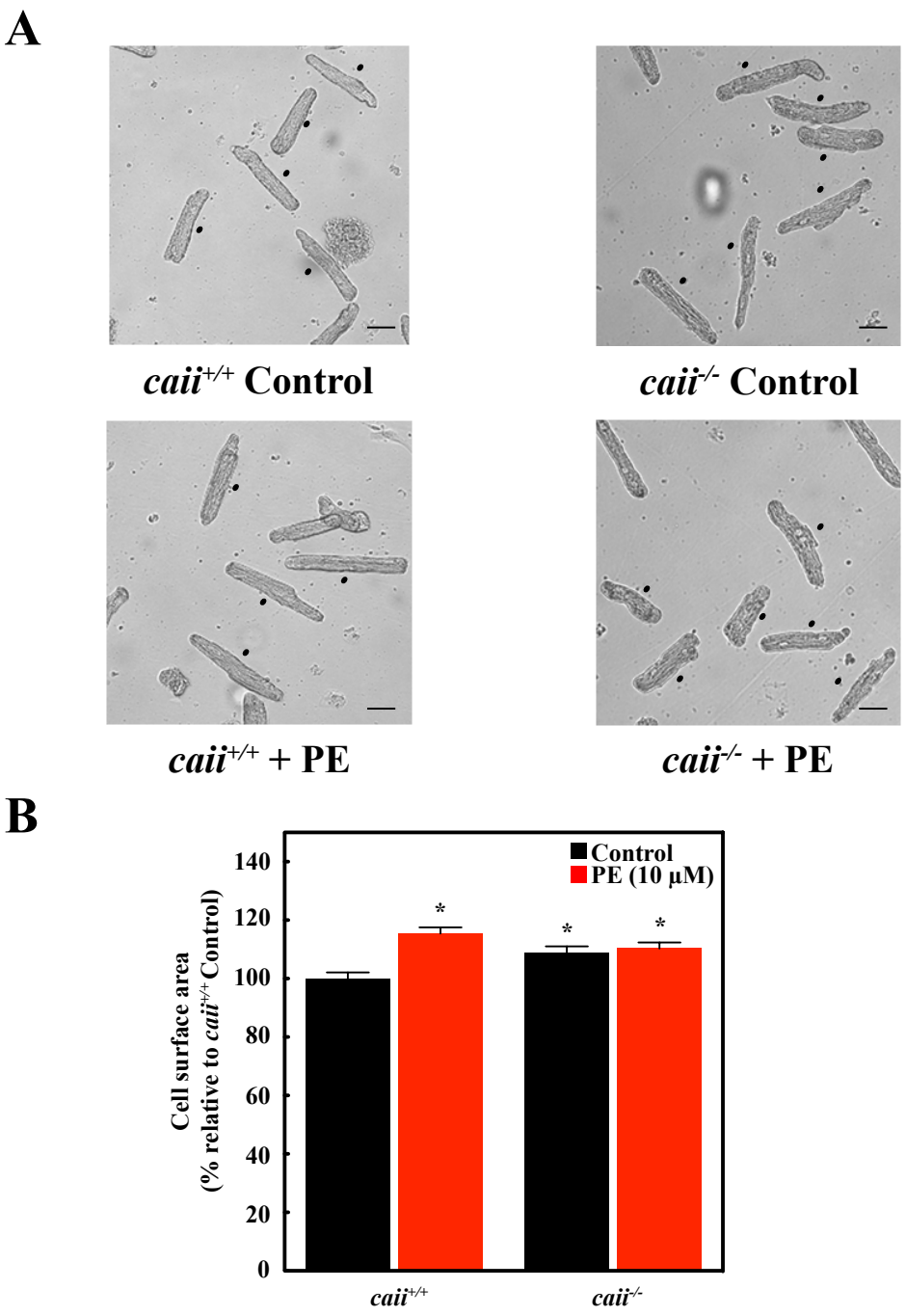

Figure 4.1. Effect of PE on the cell surface area of cultured adult mouse ventricular myocytes from wild type and *caii*$^{-/-}$ mice

(A) Images of cultured adult mouse myocytes from wild type and *caii*$^{-/-}$ mice. Scale bars are 50 µm. Cells were treated after 18 h of culture with 10 µM PE or vehicle for another 24 h. Images were collected after the 24 h treatment. Examples of cells used for cell surface area measurement are indicated by a black dot. *(B)* Cell surface areas were measured; red bars represent PE treatment groups. Values are mean ± S.E.M., n=3 trials (total cells analysed in each group, 120-180). *P < 0.05, compared with *caii*$^{+/+}$ control.

4.2.4 Effect of phenylephrine on protein synthesis in cultured cardiomyocytes from *caii*$^{-/-}$ mice

An increase in protein synthesis is an adaptive response to decreased cardiac function as a result of cardiovascular disease. To determine if CAII ablation affects protein synthesis in *caii*$^{-/-}$ mice, cardiomyocytes were incubated in the presence of [^{3}H]phenylalanine, which was added at the same time as vehicle or PE. Proteins were precipitated 24 h later using TCA, and counted in a liquid scintillation counter. While not significant, PE induced an increase in protein synthesis in cardiomyocytes isolated from wild type mice (Fig. 4.2). This effect was absent in *caii*$^{-/-}$ mice, suggesting that CAII ablation prevents PE-induced increases in protein synthesis.

4.2.5 Effect of phenylephrine on hypertrophic gene expression in cultured cardiomyocytes from *caii*$^{-/-}$ mice

As previously mentioned, reactivation of the fetal gene program in the heart is indicative of cardiac hypertrophy. qPCR was used to determine any differences in hypertrophic marker transcript abundance between wild type and *caii*$^{-/-}$ mice. To establish if CAII ablation has an effect on the other members of the hypertrophic transport metabolon, the transcript abundances of AE3fl and NHE1 were also quantified.

Cardiomyocytes from wild type mice failed to exhibit an increase in ANP, BNP, and β-MHC transcript abundance in the presence of PE (Fig 4.3A-C). Since this is not representative of what had been published previously, it is difficult to draw any definite conclusions from this data – instead, we can speculate on possible trends. The data indicates a tendency for natriuretic peptide transcript abundance to increase in myocytes from *caii*$^{-/-}$ mice, although this increase is not significantly different from wild type mice (Fig. 4.3A-B). There is no apparent difference in β-MHC transcript abundance between the two lines of mice (Fig. 4.3C).

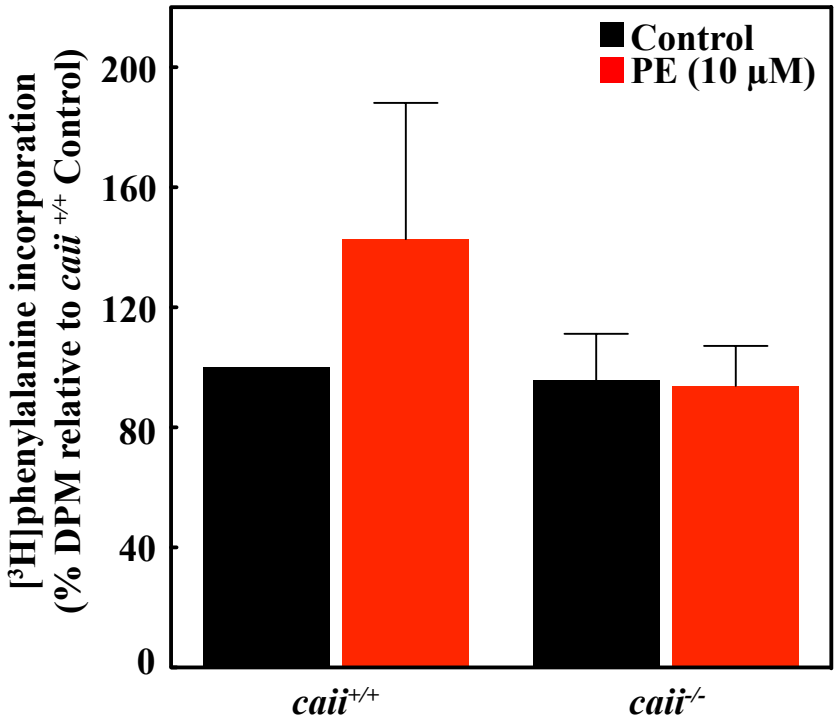

Figure 4.2. Effect of PE on the rate of protein synthesis in cultured adult mouse ventricular myocytes from wild type and *caii*$^{-/-}$ mice

Cultured adult mouse myocytes from wild type and *caii*$^{-/-}$ mice were treated after 18 h of culture with 10 µM phenylephrine (PE) or vehicle in the presence of [^{3}H]phenylalanine. Incorporated [^{3}H] was quantified after 24 h. Values are mean ± S.E.M., n = 3 trials. *P < 0.05, compared with *caii*$^{+/+}$ control.

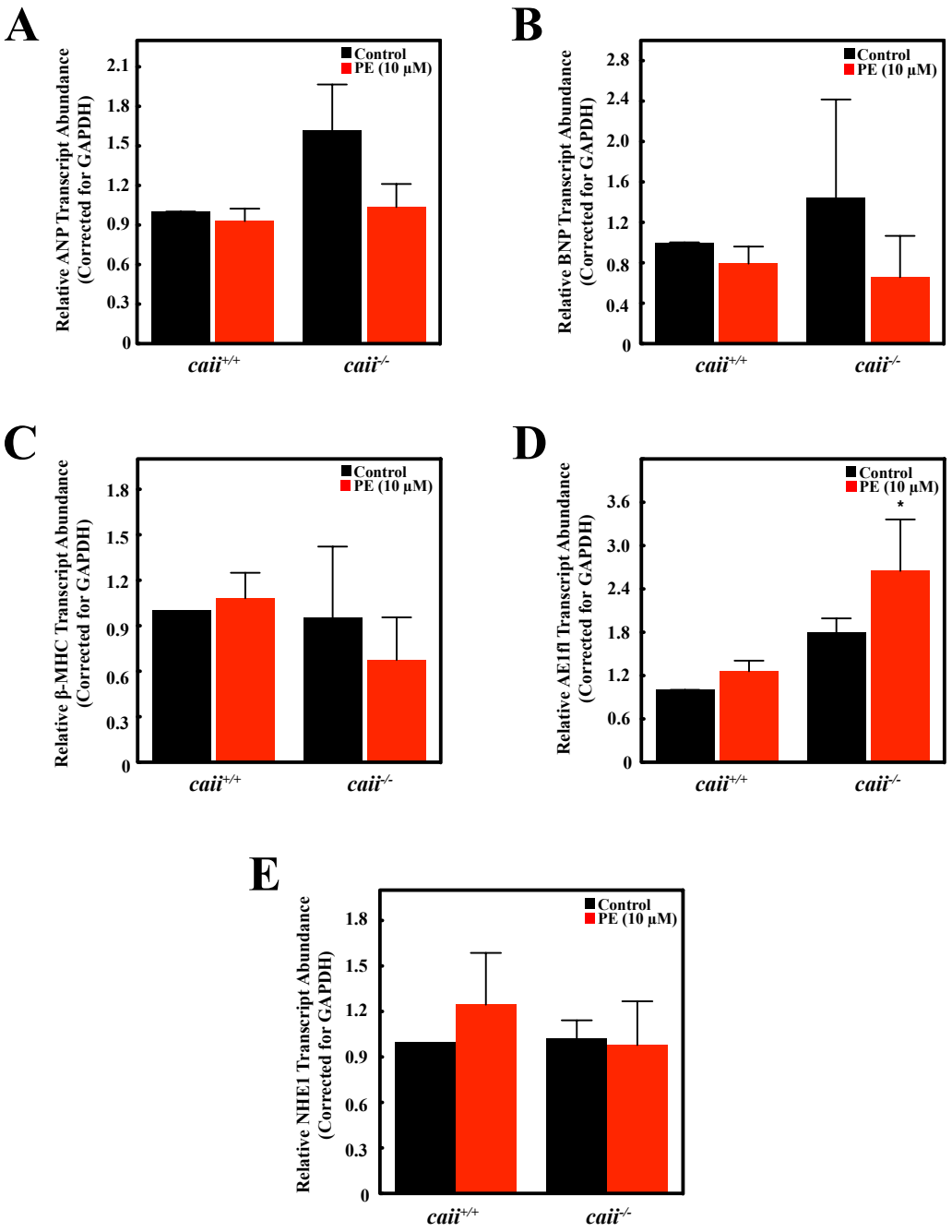

Figure 4.3. Effect of PE on hypertrophic marker and transporter transcript expression in cultured adult mouse ventricular myocytes from wild type and *caii*$^{-/-}$ mice

qPCR analysis of *(A)* ANP, *(B)* BNP, *(C)* β-MHC, *(D)* AE3fl, and *(E)* NHE1 mRNA expression in cultured rat neonatal myocytes. Data were corrected for variation using GAPDH expression and results are expressed as transcript expression normalized to GAPDH. Values are mean ± S.E.M., n = 3 for each treatment group. *P < 0.05, compared with *caii*$^{+/+}$ control.

Regarding the proteins involved in the hypertrophic transport metabolon, an increase in AE3fl transcript abundance is evident in cardiomyocytes form *caii*$^{-/-}$ mice compared to wild type, and this increase is almost 3-fold and significant in the presence of PE (Fig. 4.3D). NHE1 transcript abundance, unlike that of AE3fl, was not affected by CAII ablation or the presence of PE (Fig. 4.3E).

4.3 Discussion

Another approach to elucidate the importance of CAII in cardiomyocyte hypertrophy is the characterization of *caii*$^{-/-}$ mice. Combined analysis of heart weight/body weight ratios, left ventricular mass, echocardiographic measurements of ventricular wall dimensions, and cell surface areas reveal that the hearts of *caii*$^{-/-}$ mice exhibit hypertrophy. The fact that this hypertrophy is not accompanied by decreased cardiac function, and actually increases ejection fraction and fractional shortening, suggests that it is physiological versus pathological. *Caii*$^{-/-}$ mice manifest vascular calcification, which would likely reduce their vascular compliance (120). The physiological hypertrophy we observed in *caii*$^{-/-}$ mice may be secondary to this decrease in vascular compliance. .

The main question is whether *caii*$^{-/-}$ mice are susceptible to pathological cardiomyocyte hypertrophy. CAII inhibition and CAII over-expression studies propose that CAII is a potential pharmacological target in the treatment of heart failure. Based on this previous data, one would hypothesize that *caii*$^{-/-}$ mice are unable to sustain continuous activation of the hypertrophic transport metabolon, and therefore are protected from hypertrophy. Discerning whether PE will induce hypertrophy in cardiomyocytes isolated from *caii*$^{-/-}$ mice will partially answer this question – further experiments *in vivo* will complete the story.

Both cell surface area and protein synthesis were unaffected by the presence of PE in cardiomyocytes from *caii*$^{-/-}$ mice, compared to vehicle treated myocytes. This data suggests that CAII ablation is indeed protective from hypertrophy. It should be noted that the cell surface area of *caii*$^{-/-}$ mice cardiomyocytes is significantly larger than that of wild type mice, but this

complements the previous observation that there are increases, although not significant, in whole heart and ventricular dimensions. What is important is that PE does not induce an even greater increase in cell surface area in these myocytes compared to vehicle treated myocytes

Our experiments failed to reproduce PE-induced increases in ANP, BNP, and β-MHC transcript abundances in cardiomyocytes isolated from wild type mice. Reactivation of these fetal genes is a hallmark indicator of hypertrophy, and since PE was not successful in inducing expression of hypertrophic markers in control myocytes, interpretation of any of the PE data from the qPCR experiments needs to be made with caution.

It is interesting that vehicle-treated cardiomyocytes from *caii*$^{-/-}$ mice show a non-significant trend of increased natriuretic peptide transcript abundance compared to vehicle-treated myocyte from wild type mice, since this is normally indicative of hypertrophy. While the increase in cell surface area could also be an indication of hypertrophy, the absence of an increase in protein synthesis and the maintenance of normal cardiac function complicate this interpretation. One explanation is that ANP and BNP are exerting anti-hypertrophic effects to sustain physiological hypertrophy and prevent the progression to pathological hypertrophy. As mentioned previously, there can be a disconnect between fetal gene reactivation and other hypertrophic pathways, which can also account for discrepancies in the data. β-MHC transcript abundance was unaffected by mouse genotype, but this does not necessarily reflect any hypertrophic tendencies, as discussed previously.

We assessed the effect of CAII ablation on the other members of the hypertrophic transport metabolon, AE3fl and NHE1. AE3fl transcript abundance was increased, although not significantly, in cardiomyocytes from *caii*$^{-/-}$ mice compared to wild type mice. This increase was significant compared to myocytes from *caii*$^{+/+}$ mice in the presence of PE. This might be to accommodate the absence of CAII, to maintain and/or increase HCO_3^- extrusion in the absence of a continuous supply of substrate at the plasma membrane. An increase in the transcript abundance of NHE1 in *caii*$^{-/-}$ mice would further substantiate this idea,

but NHE1 transcript abundance was unaffected by genotype or the presence of PE.

Previously it was speculated that ETZ might attenuate hypertrophy by acting through a target other than CAII. This study demonstrates that CAII is at least one of the targets of ETZ, since the cardiomyocytes isolated from *caii*$^{-/-}$ mice were not subject to pathological hypertrophy. If it were exclusively another isoform of carbonic anhydrase responsible for promoting hypertrophy, these mice would not have been protected. The fact that AE3fl transcript abundance is higher in *caii*$^{-/-}$ mice though, which wasn't observed in CAII inhibition experiments, suggests that there might be other proteins or pathways affected by treatment with ETZ, or by a whole body knockout of CAII. Overall, indication that CAII is a target of ETZ further supports the potential use of this membrane permeant drug in the prevention or reversion of hypertrophy.

Chapter 5: Summary and Future Directions

5.1 Summary

The objective of this thesis was to explore the role of CAII in cardiomyocyte hypertrophy. Previous studies revealed that CAII inhibition prevents and reverts hypertrophy by limiting the amount of substrate available to NHE1 and AE3, thereby reducing transport activity. Further manipulation of CAII expression and activity, by means of over-expression and complete ablation *in vitro*, provided additional insight into the role of CAII in the hypertrophic transport metabolon, as well as its potential as a pharmacological target in treating heart failure. Hypertrophic markers (cell size, protein synthesis, and hypertrophic gene expression) were monitored in neonatal rat ventricular myocytes over-expressing wild type or catalytically inactive CAII. Also, cardiovascular parameters were characterized from a line of mice with a null mutation in the CAII gene, and the same hypertrophic markers were monitored in cardiomyocytes isolated from these mice in the presence of hypertrophic agonists. Specifically, we wanted to determine the effect of over-expressing CAII, or ablation of CAII, on phenylephrine-induced hypertrophy in cardiomyocytes.

Over-expression of either wild type or catalytically inactive CAII in cardiomyocytes did not affect cell size, protein synthesis, or hypertrophic gene expression compared to untreated cells. This suggests that the transport activities of AE3 and NHE1 are saturated in the presence of the endogenous CAII, and that enough is present to even prevent an effect of the dominant negative mutant. Cardiomyocytes over-expressing CAII-V143Y though did not respond in terms of cell surface area and protein synthesis to hypertrophic stimuli, which suggests that the mutant CAII behaves in a dominant negative fashion to suppress phenylephrine-induced hypertrophy. Natriuretic peptide transcript abundance was unaffected by the presence of PE, which means that they might instead be affected at the protein level, that they are exerting anti-hypertrophic effects, or there is a disconnect between reactivation of the fetal gene program and other hypertrophic pathways. The other members of the hypertrophic transport metabolon, AE3 and NHE1, were also unaffected at the transcript level by CAII over-expression or the

presence of PE, which makes sense considering there was no increase in hypertrophic markers upon over-expression of wild type CAII.

Caii$^{-/-}$ mice exhibit characteristics of physiological hypertrophy, such as increased left ventricular wall dimensions, accompanied by larger myocyte surface areas, without any decrease in systolic and diastolic cardiac function. They were also protected from hypertrophic stimulation in that PE failed to induced increases in cell surface area and protein synthesis. Non-significant increases in natriuretic peptide transcript abundances were detected in cardiomyocytes from *caii*$^{-/-}$ mice, suggesting that perhaps natriuretic peptides were exerting anti-hypertrophic effects to prevent a progression to pathological hypertrophy.

Overall, these findings continue to support a role of CAII and the rest of the hypertrophic transport metabolon in promoting cardiomyocyte hypertrophy. Experiments looking at the effect of CAII over-expression, ablation, and inhibition in response to hypertrophic stimuli *in vivo* will complete this story, and ascertain the therapeutic potential of CAII inhibition in cardiomyocyte hypertrophy and heart failure.

5.2 Future Directions

The importance of CAII and the hypertrophic metabolon in the development of cardiomyocyte hypertrophy has been well established *in vitro*. The next step in this research is to perform experiments *in vivo*, and determine the effect of CAII inhibition, and ablation, in live animals. There have already been studies using NHE1 inhibitors in whole animal models, and with considerable success. A diet of the NHE1 inhibitor cariporide attenuated increases in left ventricular end diastolic pressure, heart weight/body weight ratio, and cell size in male Sprague-Dawley rats subsequently subjected to coronary artery ligation (CAL) (144). In a similar experiment, animals that received the CAL procedure and then were fed cariporide diets were partially protected from increases in left ventricular end diastolic pressure, left ventricular dilation, and hypertrophy

compared to animals that were not fed cariporide (59). Another NHE1 inhibitor, BIIB723, fed to Wistar rats in their drinking water, prevented isoproterenol-induced increases in left ventricular mass, heart weight/body weight ratio, cardiomyocyte size, and fibrosis (31).

Our data, and the fact that CAII physically and functionally interacts with NHE1, provide support for the idea that CAII inhibition and ablation will prevent hypertrophy *in vivo*. An appropriate model in which to test CAII inhibitors would be a mouse transverse aortic constriction (TAC) model, which induces hypertension, followed by cardiac remodeling and hypertrophy (17). Regarding which CAII inhibitor to use, ETZ has proven to be a promising candidate in that it is already used clinically as a diuretic (83), and it prevented and reverted cardiomyocyte hypertrophy *in vitro* (4). Administration of ETZ to the drinking water prior to, or after administration of TAC, and then analysis of heart weight/body weight ratio, myocyte size, ventricular cavity/wall dimensions, and cardiac function will determine if ETZ is an effective inhibitor of hypertrophy in a live mouse model.

Similar experiments can be performed using the *caii*$^{-/-}$ mice to ascertain whether these mice are protected from hypertrophy. Ideally we would use a line of mice with a heart-specific knockout of *caii*, since there could be effects other than just renal tubular acidosis in our current line of whole body *caii* knockouts. All the same, an assessment of the extent of hypertrophy in *caii*$^{-/-}$ mice will provide valuable information regarding the importance of CAII in hypertrophy *in vivo*.

AE3 is also an essential component of the hypertrophic transport metabolon, and it could potentially play a role in cardiomyocyte hypertrophy as well. It is an attractive therapeutic target in that its expression is more restrictive than that of CAII (28), and it is located on the cell surface versus in the cytosol. These circumstances might reduce any side effects associated with inhibition of AE3 in a number of tissues, or membrane permeable inhibitors. Unpublished data from our lab shows that hearts from *ae3*$^{-/-}$ mice are smaller than those from wild type mice, and that cardiomyocytes from these mice are protected from

hypertrophic stimulation in that there are no increases in cell surface area, rate of protein synthesis, or ANP and β-MHC transcript abundance. These data suggest that AE3 is a potential therapeutic target in heart failure as well, which should be further explored with *in vivo* experiments similar to those suggested for CAII.

Assessment of the role of AE3 in cardiomyocyte hypertrophy is incomplete without inhibition studies, yet there are currently no specific inhibitors of AE3. Our lab is planning to develop a high throughput assay to screen a vast number of compounds for their effect on Cl^-/HCO_3^- transport activity in AE3-transfected HEK293 cells. Once specific AE3 inhibitors have been identified, the effect of AE3 inhibition on cardiomyocyte hypertrophy can be studied *in vitro*. These experiments would proceed just as those with CAII, with endpoints of cell surface area, protein synthesis, and hypertrophic gene expression. Eventually, these inhibitors can also be tested *in vivo* as well.

So far our recent exploration of the different components of the hypertrophic transport metabolon has led us down an exciting path. Investigation of the effect of CAII over-expression *in vitro*, as well as initial characterization of *caii*$^{-/-}$ and *ae3*$^{-/-}$ mice have indicated that both CAII and AE3 are important proteins in the progression of hypertrophy. Assessment of hypertrophy in these mice *in vivo*, as well as inhibition studies with ETZ and novel inhibitors of AE3 will provide a more complete story of the potential of CAII and AE3 as pharmacological targets in the treatment of heart failure.

Bibliography

1. **Alper SL.** Genetic diseases of acid-base transporters. *Annu Rev Physiol* 64: 899-923, 2002.

2. **Alvarez B, Loiselle FB, C.T S, Schwartz GJ, and Casey JR.** Direct extracellular interaction between carbonic anhydrase IV and the NBC1 Na^+/HCO_3^- co-transporter. *Biochemistry* 42: 2321-2329, 2003.

3. **Alvarez BV, Fujinaga J, and Casey JR.** Molecular basis for angiotensin II-induced increase of chloride/bicarbonate exchange in the myocardium. *Circ Research* 89: 1246-1253, 2001.

4. **Alvarez BV, Johnson DE, Sowah D, Soliman D, Light PE, Xia Y, Karmazyn M, and Casey JR.** Carbonic anhydrase inhibition prevents and reverts cardiomyocyte hypertrophy. *J Physiol* 579: 127-145, 2007.

5. **Alvarez BV, Kieller DM, Quon AL, Markovich D, and Casey JR.** Slc26a6: a cardiac chloride-hydroxyl exchanger and predominant chloride-bicarbonate exchanger of the mouse heart. *J Physiol* 561: 721-734, 2004.

6. **Alvarez BV, Vilas GL, and Casey JR.** Metabolon disruption: a mechanism that regulates bicarbonate transport. *EMBO J* 24: 2499-2511, 2005.

7. **An H, Tu C, Duda D, Montanez-Clemente I, Math K, Laipis PJ, McKenna R, and Silverman DN.** Chemical rescue in catalysis by human carbonic anhydrases II and III. *Biochemistry* 41: 3235-3242, 2002.

8. **Antos CL, McKinsey Ta, Frey N, Kutschke W, McAnally J, Shelton JM, Richardson Ja, Hill Ja, and Olson EN.** Activated glycogen synthase-3 beta suppresses cardiac hypertrophy in vivo. *Proc Natl Acad Sci U S A* 99: 907-912, 2002.

9. **Avkiran M and Marber MS.** Na^+/H^+ exchange inhibitors for cardioprotective therapy: progress, problems and prospects. *Journal of the American College of Cardiology* 39: 747-753, 2002.

10. **Baartscheer A and van Borren MMGJ.** Sodium ion transporters as new therapeutic targets in heart failure. *Cardiovasc Hematol Agents Med Chem* 6: 229-236, 2008.

11. **Barry SP, Davidson SM, and Townsend PA.** Molecular regulation of cardiac hypertrophy. *Int J Biochem Cell Biol* 40: 2023-2039, 2008.

12. **Becker HM and Deitmer JW.** Carbonic Anhydrase II increases the activity of the human electrogenic Na^+/HCO_3^- cotransporter. *J Biol Chem* 282: 13508-13521, 2007.

13. **Becker HM and Deitmer JW.** Nonenzymatic proton handling by carbonic anhydrase II during H^+-lactate cotransport via monocarboxylate transporter 1. *J Biol Chem* 283: 21655-21667, 2008.

14. **Becker HM, Hirnet D, Fecher-Trost C, Sültemeyer D, and Deitmer JW.** Transport activity of MCT1 expressed in Xenopus oocytes is increased by interaction with carbonic anhydrase. *The Journal of Biological Chemistry* 280: 39882-39889, 2005.

15. **Becker HM, Klier M, and Deitmer JW.** Nonenzymatic augmentation of lactate transport via monocarboxylate transporter isoform 4 by carbonic anhydrase II. *The Journal of Membrane Biology* 234: 125-135, 2010.

16. **Becker HM, Klier M, Schüler C, McKenna R, and Deitmer JW.** Intramolecular proton shuttle supports not only catalytic but also noncatalytic function of carbonic anhydrase II. *Proceedings of the National Academy of Sciences of the United States of America* 108: 3071-3076, 2011.

17. **Bodiga S, Zhong JC, Wang W, Basu R, Lo J, Liu GC, Guo D, Holland SM, Scholey JW, Penninger JM, Kassiri Z, and Oudit GY.** Enhanced susceptibility to biomechanical stress in ACE2 null mice is prevented by loss of the p47(phox) NADPH oxidase subunit. *Cardiovascular Research* 91: 151-161, 2011.

18. **Bogoyevitch MA, Fuller SJ, and Sugden PH.** cAMP and protein synthesis in isolated adult rat heart preparations. *Am J Physiol* 265: C1247-C1257, 1993.

19. **Boluyt MO, Zheng JS, Younes A, Long X, O'Neill L, Silverman H, Lakatta EG, and Crow MT.** Rapamycin inhibits alpha 1-adrenergic receptor-stimulated cardiac myocyte hypertrophy but not activation of hypertrophy-associated genes. Evidence for involvement of p70 S6 kinase. *Circulation Research* 81: 176-186, 1997.

20. **Boron WF.** Evaluating the role of carbonic anhydrases in the transport of HCO_3^--related species. *Biochimica et Biophysica Acta* 1804: 410-421, 2010.

21. **Bueno OF, De Windt LJ, Tymitz KM, Witt SA, Kimball TR, Klevitsky R, Hewett TE, Jones SP, Lefer DJ, Peng CF, Kitsis RN, and Molkentin JD.** The MEK1-ERK1/2 signaling pathway promotes compensated cardiac hypertrophy in transgenic mice. *EMBO J* 19: 6341-6350., 2000.

22. **Bueno OF, Wilkins BJ, Tymitz KM, Glascock BJ, Kimball TF, Lorenz JN, and Molkentin JD.** Impaired cardiac hypertrophic response in Calcineurin Aβ -deficient mice. *Proc Natl Acad Sci U S A* 99: 4586-4591, 2002.

23. **Cameron VA and Ellmers LJ.** Minireview: natriuretic peptides during development of the fetal heart and circulation. *Endocrinology* 144: 2191-2194, 2003.

24. **Cartwright EJ, Mohamed T, Oceandy D, and Neyses L.** Calcium signaling dysfunction in heart disease. *BioFactors (Oxford, England)* 37: 175-181, 2011.

25. **Casey JR.** Why bicarbonate? *Biochemistry and Cell Biology* 84: 930-939, 2006.

26. **Casey JR, Sly WS, Shah GN, and Alvarez BV.** Bicarbonate homeostasis in excitable tissues: role of AE3 Cl^-/HCO_3^- exchanger and carbonic anhydrase XIV interaction. *American Journal of Physiology Cell Physiology* 297: C1091-1102, 2009.

27. **Choukroun G, Hajjar R, Fry S, del Monte F, Haq S, Guerrero JL, Picard M, Rosenzweig a, and Force T.** Regulation of cardiac hypertrophy in vivo by the stress-activated protein kinases/c-Jun NH_2-terminal kinases. *The Journal of Clinical Investigation* 104: 391-398, 1999.

28. **Cordat E and Casey JR.** Bicarbonate transport in cell physiology and disease. *The Biochemical Journal* 417: 423-439, 2009.

29. **Counillon L and Pouysségur J.** The expanding family of eucaryotic Na^+/H^+ exchangers. *J Biol Chem* 275: 1-1, 2000.

30. **Dorn GW.** Protein kinase cascades in the regulation of cardiac hypertrophy. *J Clin Invest* 115, 2005.

31. **Ennis IL, Escudero EM, Console GM, Camihort G, Dumm CG, Seidler RW, Camilion de Hurtado MC, and Cingolani HE.** Regression of isoproterenol-induced cardiac hypertrophy by Na^+/H^+ exchanger inhibition. *Hypertension* 41: 1324-1329, 2003.

32. **Feng JA, Perry G, Mori T, Hayashi T, Oparil S, and Chen Y-F.** Pressure-independent enhancement of cardiac hypertrophy in atrial natriuretic peptide-deficient mice. *Clinical and Experimental Pharmacology & Physiology* 30: 343-349, 2003.

33. **Ferreira JCB, Brum PC, and Mochly-Rosen D.** βIIPKC and εPKC isozymes as potential pharmacological targets in cardiac hypertrophy and heart failure. *Journal of molecular and cellular cardiology*, 2010.

34. **Ferry JG.** The γ class of carbonic anhydrases. *Biochimica et Biophysica Acta* 1804: 374-381, 2010.

35. **Fiedler B, Lohmann SM, Smolenski A, Linnemuller S, Pieske B, Schroder F, Molkentin JD, Drexler H, and Wollert KC.** Inhibition of calcineurin-NFAT hypertrophy signaling by cGMP-dependent protein kinase type I in cardiac myocytes. *Proceedings of the National Academy of Sciences of the United States of America* 99: 11363-11368, 2002.

36. **Fliegel L.** Molecular biology of the myocardial Na^+/H^+ exchanger. *J Mol Cell Cardiol* 44: 228-237, 2008.

37. **Frey N and Olson EN.** Cardiac hypertrophy: the good, the bad, and the ugly. *Annu Rev Physiol* 65: 45-79, 2003.

38. **Fujikawa-Adachi K, Nishimori I, Taguchi T, and Onishi S.** Human carbonic anhydrase XIV (CA14): cDNA cloning, mRNA expression, and mapping to chromosome 1. *Genomics* 61: 74-81, 1999.

39. **Gadde KM, Franciscy DM, Wagner HR, and Krishnan KRR.** Zonisamide for weight loss in obese adults: a randomized controlled trial. *JAMA : The Journal of the American Medical Association* 289: 1820-1825, 2003.

40. **Gardner DG, Chen S, Glenn DJ, and Grigsby CL.** Molecular biology of the natriuretic peptide system: implications for physiology and hypertension. *Hypertension* 49: 419-426, 2007.

41. **Halestrap AP and Meredith D.** The SLC16 gene family-from monocarboxylate transporters (MCTs) to aromatic amino acid transporters and beyond. *Pflügers Archiv : European Journal of Physiology* 447: 619-628, 2004.

42. **Harris IS, Zhang S, Treskov I, Kovacs A, Weinheimer C, and Muslin AJ.** Raf-1 kinase is required for cardiac hypertrophy and cardiomyocyte survival in response to pressure overload. *Circulation* 110: 718-723, 2004.

43. **Hayasaki-Kajiwara Y, Kitano Y, Iwasaki T, Shimamura T, Naya N, Iwaki K, and Nakajima M.** Na^+ influx via Na^+/H^+ exchange activates protein kinase C isozymes delta and epsilon in cultured neonatal rat cardiac myocytes. *J Mol Cell Cardiol* 31: 1559-1572., 1999.

44. **He TC, Zhou S, da Costa LT, Yu J, Kinzler KW, and Vogelstein B.** A simplified system for generating recombinant adenoviruses. *Proc Natl Acad Sci U S A* 95: 2509-2514, 1998.

45. **Hilvo M, Salzano AM, Innocenti A, Kulomaa MS, Scozzafava A, Scaloni A, Parkkila S, and Supuran CT.** Cloning, expression, post-translational modifications and inhibition studies on the latest mammalian carbonic anhydrase isoform, CA XV. *Journal of Medicinal Chemistry* 52: 646-654, 2009.

46. **Hunter JJ, Tanaka N, Rockman Ha, Ross J, and Chien KR.** Ventricular expression of a MLC-2v-ras fusion gene induces cardiac hypertrophy

and selective diastolic dysfunction in transgenic mice. *The Journal of Biological Chemistry* 270: 23173-23178, 1995.

47. **Johnson DE and Casey JR.** Cytosolic H^+ microdomain developed around AE1 during AE1-mediated Cl^-/HCO_3^- exchange. *The Journal of Physiology* 589: 1551-1569, 2011.

48. **Kaiser Ra, Liang Q, Bueno O, Huang Y, Lackey T, Klevitsky R, Hewett TE, and Molkentin JD.** Genetic inhibition or activation of JNK1/2 protects the myocardium from ischemia-reperfusion-induced cell death in vivo. *The Journal of Biological Chemistry* 280: 32602-32608, 2005.

49. **Karmazyn M, Liu Q, Gan XT, Brix BJ, and Fliegel L.** Aldosterone increases NHE-1 expression and induces NHE-1-dependent hypertrophy in neonatal rat ventricular myocytes. *Hypertension* 42: 1171-1176, 2003.

50. **Kemp G, Young H, and Fliegel L.** Structure and function of the human Na^+/H^+ exchanger isoform 1. *Channels (Austin, Tex)* 2: 329-336, 2008.

51. **Khandoudi N, Albadine J, Robert P, Krief S, Berrebi-Bertrand I, Martin X, Bevensee MO, Boron WF, and Bril A.** Inhibition of the cardiac electrogenic sodium bicarbonate cotransporter reduces ischemic injury. *Cardiovasc Res* 52: 387-396, 2001.

52. **Kifor G, Toon MR, Janoshazi A, and Solomon AK.** Interaction between red cell membrane band 3 and cytosolic carbonic anhydrase. *J Membr Biol* 134: 169-179, 1993.

53. **Kilic A, Velic A, De Windt LJ, Fabritz L, Voss M, Mitko D, Zwiener M, Baba HA, van Eickels M, Schlatter E, and Kuhn M.** Enhanced activity of the myocardial Na^+/H^+ exchanger NHE-1 contributes to cardiac remodeling in atrial natriuretic peptide receptor-deficient mice. *Circulation* 112: 2307-2317., 2005.

54. **Kishimoto I, Rossi K, and Garbers DL.** A genetic model provides evidence that the receptor for atrial natriuretic peptide (guanylyl cyclase-A) inhibits cardiac ventricular myocyte hypertrophy. *Proceedings of the National Academy of Sciences of the United States of America* 98: 2703-2706, 2001.

55. **Klee CB, Ren H, and Wang X.** Regulation of the calmodulin-stimulated protein phosphatase, calcineurin. *The Journal of Biological Chemistry* 273: 13367-13370, 1998.

56. **Klier M, Schüler C, Halestrap AP, Sly WS, Deitmer JW, and Becker HM.** Transport activity of the high-affinity monocarboxylate transporter MCT2 is enhanced by extracellular carbonic anhydrase IV but not by intracellular carbonic anhydrase II. *The Journal of Biological Chemistry*, 2011.

57. **Knowles JW, Esposito G, Mao L, Hagaman JR, Fox JE, Smithies O, Rockman Ha, and Maeda N.** Pressure-independent enhancement of cardiac hypertrophy in natriuretic peptide receptor A-deficient mice. *The Journal of Clinical Investigation* 107: 975-984, 2001.

58. **Kovacic S, Soltys C-LM, Barr AJ, Shiojima I, Walsh K, and Dyck JRB.** Akt activity negatively regulates phosphorylation of AMP-activated protein kinase in the heart. *J Biol Chem* 278: 39422-39427, 2003.

59. **Kusumoto K, Haist JV, and Karmazyn M.** Na^+/H^+ exchange inhibition reduces hypertrophy and heart failure after myocardial infarction in rats. *Am J Physiol Heart Circ Physiol* 280: H738-745., 2001.

60. **Lane TW, Saito MA, George GN, Pickering IJ, Prince RC, and Morel FMM.** Biochemistry: a cadmium enzyme from a marine diatom. *Nature* 435: 42-42, 2005.

61. **Lewis SE, Erickson RP, Barnett LB, Venta PJ, and Tashian RE.** N-ethyl-N-nitrosourea-induced null mutation at the mouse Car-2 locus: an animal model for human carbonic anhydrase II deficiency syndrome. *Proc Natl Acad Sci U S A* 85: 1962-1966, 1988.

62. **Li X, Alvarez B, Casey JR, Reithmeier RAF, and Fliegel L.** Carbonic anhydrase II binds to and enhances activity of the Na^+/H^+ exchanger. *J Biol Chem* 277: 36085-36085, 2002.

63. **Liang Q, Bueno OF, Wilkins BJ, Kuan C-Y, Xia Y, and Molkentin JD.** c-Jun N-terminal kinases (JNK) antagonize cardiac growth through cross-talk with calcineurin-NFAT signaling. *The EMBO Journal* 22: 5079-5089, 2003.

64. **Liao P, Georgakopoulos D, Kovacs a, Zheng M, Lerner D, Pu H, Saffitz J, Chien K, Xiao RP, Kass Da, and Wang Y.** The in vivo role of p38 MAP kinases in cardiac remodeling and restrictive cardiomyopathy. *Proceedings of the National Academy of Sciences of the United States of America* 98: 12283-12288, 2001.

65. **Link AJ and Labaer J.** Trichloroacetic Acid (TCA) Precipitation of Proteins. *Cold Spring Harbor Protocols* 2011: 993-994, 2011.

66. **Liu W, Zi M, Jin J, Prehar S, Oceandy D, Kimura TE, Lei M, Neyses L, Weston AH, Cartwright EJ, and Wang X.** Cardiac-specific deletion of mkk4 reveals its role in pathological hypertrophic remodeling but not in physiological cardiac growth. *Circulation Research* 104: 905-914, 2009.

67. **Loiselle FB, Alvarez BV, and Casey JR.** Regulation of the Human NBC3 Na^+/HCO_3^- co-transporter by Carbonic Anhydrase II and Protein Kinase A. *Am J Physiol* 286: 307-317, 2004.

68. **López JE, Myagmar B-E, Swigart PM, Montgomery MD, Haynam S, Bigos M, Rodrigo MC, and Simpson PC.** β-Myosin Heavy Chain Is Induced by Pressure Overload in a Minor Subpopulation of Smaller Mouse Cardiac Myocytes. *Circulation Research*: 629-638, 2011.

69. **Lowes BD, Minobe W, Abraham WT, Rizeq MN, Bohlmeyer TJ, Quaife Ra, Roden RL, Dutcher DL, Robertson aD, Voelkel NF, Badesch DB, Groves BM, Gilbert EM, and Bristow MR.** Changes in gene expression in the intact human heart. Downregulation of α-myosin heavy chain in hypertrophied, failing ventricular myocardium. *The Journal of Clinical Investigation* 100: 2315-2324, 1997.

70. **Lu J, Daly CM, Parker MD, Gill HS, Piermarini PM, Pelletier MF, and Boron WF.** Effect of human carbonic anhydrase II on the activity of the human electrogenic Na/HCO_3 cotransporter NBCe1-A in Xenopus oocytes. *J Biol Chem* 281: 19241-19250, 2006.

71. **Maier LS and Bers DM.** Calcium, calmodulin, and calcium-calmodulin kinase II: heartbeat to heartbeat and beyond. *Journal of Molecular and Cellular Cardiology* 34: 919-939, 2002.

72. **Maren TH.** Carbonic anhydrase: chemistry, physiology, and inhibition. *Physiol Rev* 47: 595-781, 1967.

73. **Martinov V, Rizvi SMH, Weiseth SA, Sagave J, Bergersen LH, and Valen G.** Increased expression of monocarboxylate transporter 1 after acute ischemia of isolated, perfused mouse hearts. *Life Sciences* 85: 379-385, 2009.

74. **Maupin CM, Castillo N, Taraphder S, Tu C, McKenna R, Silverman DN, and Voth Ga.** Chemical rescue of enzymes: proton transfer in mutants of human carbonic anhydrase II. *Journal of the American Chemical Society* 133: 6223-6234, 2011.

75. **McMurtrie HL, Cleary HJ, Alvarez BV, Loiselle FB, Sterling D, Morgan PE, Johnson DE, and Casey JR.** The bicarbonate transport metabolon. *J Enzyme Inhib Med Chem* 19: 231-236., 2004.

76. **Meredith D and Christian HC.** The SLC16 monocaboxylate transporter family. *Xenobiotica* 38: 1072-1106, 2008.

77. **Miyata S, Minobe W, Bristow MR, and Leinwand La.** Myosin heavy chain isoform expression in the failing and nonfailing human heart. *Circulation Research* 86: 386-390, 2000.

78. **Moor AN and Fliegel L.** Protein kinase-mediated regulation of the Na^+/H^+ exchanger in the rat myocardium by mitogen-activated protein kinase-dependent pathways. *J Biol Chem* 274: 22985-22985, 1999.

79. **Morgan PE, Pastoreková S, Stuart-Tilley AK, Alper SL, and Casey JR.** Interactions of Transmembrane Carbonic Anhydrase, CAIX, with Bicarbonate Transporters. *Am J Physiol* 293: C738-744, 2007.

80. **Mori K, Ogawa Y, Ebihara K, Tamura N, Tashiro K, Kuwahara T, Mukoyama M, Sugawara A, Ozaki S, Tanaka I, and Nakao K.** Isolation and characterization of CA XIV, a novel membrane-bound carbonic anhydrase from mouse kidney. *J Biol Chem* 274: 15701-15705, 1999.

81. **Mori T, Chen Y-F, Feng JA, Hayashi T, Oparil S, and Perry GJ.** Volume overload results in exaggerated cardiac hypertrophy in the atrial natriuretic peptide knockout mouse. *Cardiovascular Research* 61: 771-779, 2004.

82. **Morkin E.** Control of cardiac myosin heavy chain gene expression. *Microscopy Research and Technique* 50: 522-531, 2000.

83. **Moyer JH and Ford RV.** Laboratory and clinical observations on ethoxzolamide (cardrase) as a diuretic agent. *Am J Cardiol* 1: 497-504., 1958.

84. **Mraiche F and Fliegel L.** Elevated expression of activated Na^+/H^+ exchanger protein induces hypertrophy in isolated rat neonatal ventricular cardiomyocytes. *Molecular and cellular biochemistry*, 2011.

85. **Nakao K, Minobe W, Roden R, Bristow MR, and Leinwand La.** Myosin heavy chain gene expression in human heart failure. *The Journal of Clinical Investigation* 100: 2362-2370, 1997.

86. **Nemoto S, Sheng Z, and Lin A.** Opposing Effects of Jun Kinase and p38 Mitogen-Activated Protein Kinases on Cardiomyocyte Hypertrophy. *Molecular and Cellular Biology* 18: 3518-3518, 1998.

87. **Okuyama T, Sato S, Zhu XL, Waheed A, and Sly WS.** Human carbonic anhydrase IV: cDNA cloning, sequence comparison, and expression in COS cell membranes. *Proc Natl Acad Sci U S A* 89: 1315-1319, 1992.

88. **Oudit GY and Penninger JM.** Cardiac regulation by phosphoinositide 3-kinases and PTEN. *Cardiovascular Research* 82: 250-260, 2009.

89. **Palaniyandi SS, Sun L, Ferreira JCB, and Mochly-Rosen D.** Protein kinase C in heart failure: a therapeutic target? *Cardiovascular Research* 82: 229-239, 2009.

90. **Pan P, Leppilampi M, Pastorekova S, Pastorek J, Waheed A, Sly WS, and Parkkila S.** Carbonic anhydrase gene expression in CA II-deficient (*Car2*$^{-/-}$) and CA IX-deficient (*Car9*$^{-/-}$) mice. *The Journal of Physiology* 571: 319-327, 2006.

91. **Pandya K, Kim H-S, and Smithies O.** Fibrosis, not cell size, delineates β-myosin heavy chain reexpression during cardiac hypertrophy and normal aging in vivo. *Proc Natl Acad Sci U S A* 103: 16864-16869, 2006.

92. **Pandya K and Smithies O.** β-MyHC and cardiac hypertrophy: size does matter. *Circulation Research* 109: 609-610, 2011.

93. **Pastorekova S, Parkkila S, Pastorek J, and Supuran CT.** Carbonic anhydrases: current state of the art, therapeutic applications and future prospects. *J Enzyme Inhib Med Chem* 19: 199-229, 2004.

94. **Pastorekova S and Pastorek J.** Cancer-Related Carbonic Anhydrase Isozymes and Their Inhibition. In: *Carbonic anhydrase: its inhibitors and activators*, edited by Supuran CT, Scozzafava A and Conway J. Boca Raton: CRC Press LLC, 2004.

95. **Perez NG, Alvarez BV, Camilion de Hurtado MC, and Cingolani HE.** pHi Regulation in Myocardium of the Spontaneously Hypertensive Rat: Compensated Enhanced Activity of the Na^+-H^+ Exchanger. *Circulation Research* 77: 1192-1192, 1995.

96. **Perez NG, de Hurtado MCC, and Cingolani HE.** Reverse mode of the Na^+-Ca^{2+} exchange after myocardial stretch: underlying mechanism of the slow force response. *Circulation Research* 88: 376-376, 2001.

97. **Petrich BG, Eloff BC, Lerner DL, Kovacs A, Saffitz JE, Rosenbaum DS, and Wang Y.** Targeted activation of c-Jun N-terminal kinase in vivo induces restrictive cardiomyopathy and conduction defects. *J Biol Chem* 279: 15330-15338, 2004.

98. **Picard F, Deshaies Y, Lalonde J, Samson P, and Richard D.** Topiramate reduces energy and fat gains in lean (Fa/?) and obese (fa/fa) Zucker rats. *Obesity research* 8: 656-663, 2000.

99. **Piermarini PM, Kim EY, and Boron WF.** Evidence against a direct interaction between intracellular carbonic anhydrase II and pure C-terminal domains of SLC4 bicarbonate transporters. *The Journal of Biological Chemistry* 282: 1409-1421, 2007.

100. **Pikkarainen S, Tokola H, Kerkelä R, and Ruskoaho H.** GATA transcription factors in the developing and adult heart. *Cardiovascular Research* 63: 196-207, 2004.

101. **Pushkin A, Abuladze N, Gross E, Newman D, Tatishchev S, Lee I, Fedotoff O, Bondar G, Azimov R, Ngyuen M, and Kurtz I.** Molecular mechanism of kNBC1-carbonic anhydrase II interaction in proximal tubule cells. *J Physiol* 559: 55-65, 2004.

102. **Reiser PJ, Portman MA, and Ning XH.** Human cardiac myosin heavy chain isoforms in fetal and failing adult atria and ventricles. *American Journal of*, 2001.

103. **Reiser PJ, Portman MA, Ning XH, and Moravec CS.** Human cardiac myosin heavy chain isoforms in fetal and failing adult atria and ventricles. *American Journal of Physiology-Heart and Circulatory Physiology* 280: H1814-H1814, 2001.

104. **Reithmeier RAF.** A membrane metabolon linking carbonic anhydrase with chloride/bicarbonate anion exchangers. *Blood cells, Molecules and Diseases* 27: 85-89, 2001.

105. **Riihonen R, Supuran CT, Parkkila S, Pastorekova S, Väänänen HK, and Laitala-Leinonen T.** Membrane-bound carbonic anhydrases in osteoclasts. *Bone* 40: 1021-1031, 2007.

106. **Rohini A, Agrawal N, Koyani CN, and Singh R.** Molecular targets and regulators of cardiac hypertrophy. *Pharmacological research : the official journal of the Italian Pharmacological Society* 61: 269-280, 2010.

107. **Romero MF, Fulton CM, and Boron WF.** The SLC4 family of HCO_3^- transporters. *Pflugers Arch* 447: 496-509, 2004.

108. **Rose BA, Force T, and Wang Y.** Mitogen-Activated Protein Kinase Signaling in the Heart: Angels Versus Demons in a Heart-Breaking Tale. *Physiological reviews* 90: 1507-1507, 2010.

109. **Ross H, Howlett J, Arnold JMO, Liu P, O'Neill BJ, Brophy JM, Simpson CS, Sholdice MM, Knudtson M, Ross DB, Rottger J, and Glasgow K.** Treating the right patient at the right time: Access to heart failure care. *Can J Cardiol* 22: 749-754, 2006.

110. **Rowlett RS.** Structure and catalytic mechanism of the β-carbonic anhydrases. *Biochimica et Biophysica Acta* 1804: 362-373, 2010.

111. **Sambrano GR, Fraser I, Han H, Ni Y, O'Connell T, Yan Z, and Stull JT.** Navigating the signalling network in mouse cardiac myocytes. *Nature* 420: 712-714, 2002.

112. **Scheibe RJ, Gros G, Parkkila S, Waheed A, Grubb JH, Shah GN, Sly WS, and Wetzel P.** Expression of membrane-bound carbonic anhydrases IV, IX, and XIV in the mouse heart. *J Histochem Cytochem* 54: 1379-1391, 2006.

113. **Scozzafava A and Supuran CT.** Carbonic anhydrase activators: Human isozyme II is strongly activated by oligopeptides incorporating the carboxyterminal sequence of the bicarbonate anion exchanger AE1. *Bioorg Med Chem Lett* 12: 1177-1180, 2002.

114. **Shah GN, Hewett-Emmett D, Grubb JH, Migas MC, Fleming RE, Waheed A, and Sly WS.** Mitochondrial carbonic anhydrase CA VB: differences in tissue distribution and pattern of evolution from those of CA VA suggest distinct physiological roles. *Proceedings of the National Academy of Sciences of the United States of America* 97: 1677-1682, 2000.

115. **Shioi T, Kang PM, Douglas PS, Hampe J, Yballe CM, Lawitts J, Cantley LC, and Izumo S.** The conserved phosphoinositide 3-kinase pathway determines heart size in mice. *EMBO J* 19: 2537-2548, 2000.

116. **Sly WS and Hu PY.** Human carbonic anhydrases and carbonic anhydrase deficiencies. *Annu Rev Biochem* 64: 375-401, 1995.

117. **Soleimani M and Burnham CE.** Na^+:HCO_3^- Cotransporters (NBC): Cloning and Characterization. *Journal of Membrane Biology* 183: 71-84, 2001.

118. **Soleimani M and Burnham CE.** Physiologic and molecular aspects of the Na^+:HCO_3^- cotransporter in health and disease processes. *Kidney Int* 57: 371-384, 2000.

119. **Sowah D and Casey JR.** An Intramolecular Transport Metabolon: Fusion of Carbonic Anhydrase II to the C-terminus of the Cl^-/HCO_3^- Exchanger, AE1. *American Journal of Physiology Cell physiology*, 2011.

120. **Spicer SS, Lewis SE, Tashian RE, and Schulte Ba.** Mice carrying a CAR-2 null allele lack carbonic anhydrase II immunohistochemically and show vascular calcification. *The American Journal of Pathology* 134: 947-954, 1989.

121. **Srere PA.** Complexes of sequential metabolic enzymes. *Annu Rev Biochem* 56: 89-124, 1987.

122. **Sterling D, Alvarez BV, and Casey JR.** The extracellular component of a transport metabolon. Extracellular loop 4 of the human AE1 Cl^-/HCO_3^- exchanger binds carbonic anhydrase IV. *The Journal of Biological Chemistry* 277: 25239-25246, 2002.

123. **Sterling D, Brown NJD, Supuran CT, and Casey JR.** The functional and physical relationship between the DRA bicarbonate transporter and carbonic anhydrase II. *American Journal of Physiology Cell Physiology* 283: C1522-1529, 2002.

124. **Sterling D, Reithmeier Ra, and Casey JR.** A transport metabolon. Functional interaction of carbonic anhydrase II and chloride/bicarbonate exchangers. *J Biol Chem* 276: 47886-47894, 2001.

125. **Sugden PH, Fuller SJ, Weiss SC, and Clerk A.** Glycogen synthase kinase 3 (GSK3) in the heart: a point of integration in hypertrophic signalling and

a therapeutic target? A critical analysis. *British Journal of Pharmacology* 153 Suppl: S137-153, 2008.

126. **Sun M-K and Alkon DL.** Carbonic anhydrase gating of attention: memory therapy and enhancement. *Trends in Pharmacological Sciences* 23: 83-89, 2002.

127. **Supuran CT.** Carbonic anhydrases: novel therapeutic applications for inhibitors and activators. *Nature Reviews Drug Discovery* 7: 168-181, 2008.

128. **Supuran CT, Scozzafava A, and Conway J.** *Carbonic anhydrase: its inhibitors and activators*. Boca Raton: CRC Press LLC, 2004.

129. **Tachibana H, Perrino C, Takaoka H, Davis RJ, Naga Prasad SV, and Rockman Ha.** JNK1 is required to preserve cardiac function in the early response to pressure overload. *Biochemical and Biophysical Research Communications* 343: 1060-1066, 2006.

130. **Tamura N, Ogawa Y, Chusho H, Nakamura K, Nakao K, Suda M, Kasahara M, Hashimoto R, Katsuura G, Mukoyama M, Itoh H, Saito Y, Tanaka I, Otani H, and Katsuki M.** Cardiac fibrosis in mice lacking brain natriuretic peptide. *Proceedings of the National Academy of Sciences of the United States of America* 97: 4239-4244, 2000.

131. **Theroux P, Chaitman BR, Danchin N, Erhardt L, Meinertz T, Schroeder JS, Tognoni G, White HD, Willerson JT, and Jessel A.** Inhibition of the sodium-hydrogen exchanger with cariporide to prevent myocardial infarction in high-risk ischemic situations. Main results of the GUARDIAN trial. Guard during ischemia against necrosis (GUARDIAN) Investigators. *Circulation* 102: 3032-3038, 2000.

132. **Ueyama T, Kawashima S, Sakoda T, Rikitake Y, Ishida T, Kawai M, Yamashita T, Ishido S, Hotta H, and Yokoyama M.** Requirement of activation of the extracellular signal-regulated kinase cascade in myocardial cell hypertrophy. *Journal of Molecular and Cellular Cardiology* 32: 947-960, 2000.

133. **Vaughan-Jones RD, Spitzer KW, and Swietach P.** Intracellular pH regulation in heart. *J Mol Cell Cardiol* 46: 318-331, 2009.

134. **Vaughan-Jones RD, Spitzer KW, and Swietach P.** Spatial aspects of intracellular pH regulation in heart muscle. *Prog Biophys Mol Biol* 90: 207-224, 2006.

135. **Vega RB, Yang J, Rothermel Ba, Bassel-Duby R, and Williams RS.** Multiple domains of MCIP1 contribute to inhibition of calcineurin activity. *The Journal of Biological Chemistry* 277: 30401-30407, 2002.

136. **Vince JW, Carlsson U, and Reithmeier RAF.** Localization of the Cl^-/HCO_3^- anion exchanger binding site to the amino-terminal region of carbonic anhydrase II. *Biochemistry* 39: 13344-13349, 2000.

137. **Vince JW and Reithmeier RAF.** Carbonic anhydrase II binds to the carboxyl-terminus of human band 3, the erythrocyte Cl^-/HCO_3^- exchanger. *J Biol Chem* 273: 28430-28437, 1998.

138. **Vince JW and Reithmeier RAF.** Identification of the carbonic anhydrase II binding site in the Cl^-/HCO_3^-anion exchanger AE1. *Biochemistry* 39: 5527-5533, 2000.

139. **Waheed A, Zhu XL, and Sly WS.** Membrane-associated carbonic anhydrase from rat lung. Purification, characterization, tissue distribution, and comparison with carbonic anhydrase IVs of other mammals. *Journal of Biological Chemistry* 267: 3308-3308, 1992.

140. **Waheed A, Zhu XL, Sly WS, Wetzel P, and Gros G.** Rat skeletal muscle membrane associated carbonic anhydrase is 39-kDa, glycosylated, GPI-anchored CA IV. *Arch Biochem Biophys* 294: 550-556, 1992.

141. **Wang Y, Su B, Sah VP, Brown JH, Han J, and Chien KR.** Cardiac hypertrophy induced by mitogen-activated protein kinase kinase 7, a specific activator for c-Jun NH2-terminal kinase in ventricular muscle cells. *The Journal of Biological Chemistry* 273: 5423-5426, 1998.

142. **Xu Y, Feng L, Jeffrey PD, Shi Y, and Morel FoMM.** Structure and metal exchange in the cadmium carbonic anhydrase of marine diatoms. *Nature* 452: 56-61, 2008.

143. **Yamamoto T, Shirayama T, Sakatani T, Takahashi T, Tanaka H, Takamatsu T, Spitzer KW, and Matsubara H.** Enhanced activity of ventricular Na^+-HCO_3^- cotransport in pressure-overload hypertrophy. *Am J Physiol*, 2007.

144. **Yoshida H and Karmazyn M.** Na^+/H^+ exchange inhibition attenuates hypertrophy and heart failure in 1-wk postinfarction rat myocardium. *Am J Physiol Heart Circ Physiol* 278: H300-304., 2000.

145. **Zeymer U, Suryapranata H, Monassier JP, Opolski G, Davies J, Rasmanis G, Linssen G, Tebbe U, Schröder R, Tiemann R, Machnig T, and Neuhaus KL.** The Na^+/H^+ exchange inhibitor eniporide as an adjunct to early reperfusion therapy for acute myocardial infarction. Results of the evaluation of the safety and cardioprotective effects of eniporide in acute myocardial infarction (ESCAMI) trial. *J Am Coll Cardiol* 38: 1644-1650, 2001.